

1 **Temporal dynamics of bacterial and fungal communities**  
2 **during the infection of *Brassica rapa* roots by the protist**  
3 ***Plasmodiophora brassicae***

4

5 **The impact of a pathogen on the plant root and rhizosphere microbiota**

6

7 Lionel Lebreton <sup>a\*</sup>, Anne-Yvonne Guillerm-Erckelboudt <sup>a</sup>, Kévin Gazengel <sup>a</sup>, Juliette Linglin <sup>a</sup>, Morgane  
8 Ourry <sup>a</sup>, Pascal Glory <sup>a</sup>, Alain Sarniguet <sup>a</sup>, Stéphanie Daval <sup>a</sup>, Maria J. Manzanares-Dauleux <sup>a</sup> and  
9 Christophe Mougel <sup>a</sup>

10 <sup>a</sup> IGEPP, INRA, AGROCAMPUS OUEST, Université Rennes, 35650 Le Rheu, France

11

12

13

14 \* Corresponding author:

15 E-mail: [lionel.lebreton@inra.fr](mailto:lionel.lebreton@inra.fr)

16

17

18

19

20

21

22

23

24

25

26

## 27 **Abstract**

28           The temporal dynamics of rhizosphere and root microbiota composition was compared  
29 between healthy and infected Chinese cabbage plants by the pathogen *Plasmodiophora brassicae*.  
30 When inoculated with *P. brassicae*, disease was measured at five sampling dates from early root hair  
31 infection to late gall development. The first symptoms of clubroot disease appeared 14 days after  
32 inoculation (DAI) and increased drastically between 14 and 35 DAI. The structure of microbial  
33 communities associated to rhizosphere soil and root from healthy and inoculated plants was  
34 characterized through high-throughput DNA sequencing of bacterial (16S) and fungal (18S) molecular  
35 markers and compared at each sampling date. In healthy plants, Proteobacteria and Bacteroidetes  
36 bacterial phyla dominated the rhizosphere and root microbiota of Chinese cabbage. Rhizosphere  
37 bacterial communities contained higher abundances of Actinobacteria and Firmicutes compared to  
38 the roots. Moreover, a drastic shift of fungal communities of healthy plants occurred between the  
39 two last sampling dates, especially in plant roots, where most of Ascomycota fungi dominated until  
40 they were replaced by a fungus assigned to the Chytridiomycota phylum. Parasitic invasion by *P.*  
41 *brassicae* disrupted the rhizosphere and root-associated community assembly at a late step during  
42 the root secondary cortical infection stage of clubroot disease. At this stage, *Flavisolibacter* and  
43 *Streptomyces* in the rhizosphere, and *Bacillus* in the roots, were drastically less abundant upon  
44 parasite invasion. Rhizosphere of plants colonized by *P. brassicae* was significantly more invaded by  
45 the Chytridiomycota fungus, which could reflect a mutualistic relationship in this compartment  
46 between these two microorganisms.

47

## 48 **Introduction**

49           All plant tissues including roots [1,2], leaves [3,4] and seeds [5,6] are surrounded by a large  
50 diversity of microorganisms assembled in microbial communities or microbiota. These microbial

51 assemblies represent a continuum of symbiosis with the plant ranging from parasitic to mutualistic  
52 interactions with complex microbe-microbe and microbe-plant interactions. Plant growth and health  
53 (including development, nutrition, physiology and defence) is influenced by these hosted complex  
54 microbial networks. Indeed, microbiota can stimulate seed germination and plant growth, help  
55 plants fight off disease, promote stress resistance, and influence plant fitness [7]. Thus, the plant  
56 microbiota extends the capacity of plants to adapt to their environment and contribute in shaping  
57 the plant phenotype.

58

59         Among these plant compartments, root and rhizosphere are the most studied habitats for  
60 microbial communities owing to their great potential for plant nutrition and health [1,8,9]. These  
61 microbial communities are mainly recruited by the plant from the soil [2,10,11] which is considered  
62 as the main microbial seed bank [12]. Many of these microorganisms including Archaea- and Eu-  
63 bacteria, fungi, and oomycetes live in the rhizosphere, defined as the narrow zone of soil that is  
64 influenced by root secretions [13,14]. Microbial community assemblies in the rhizosphere are  
65 governed by both abiotic and biotic factors. Soil properties, geographical location and Corine Land  
66 Cover in interaction with agronomical practices are the main factors that structure these  
67 communities [2,15,16]. Plant species and plant genotypes also determine to a lesser extent which  
68 members from the soil pool of microorganisms can grow and thrive in the rhizosphere [10,15,17,18].  
69 Plants may modulate the rhizosphere microbiota to their benefit by selectively stimulating  
70 microorganisms showing traits that are beneficial to plant growth and health [9,19]. Rhizodeposits  
71 released by plant are known to account for variations of the diversity of microbial communities in the  
72 rhizosphere [20]. The modifications of the diversity of microbial communities are then expected to  
73 mirror variations of the composition of rhizodeposits. These rhizodeposits include both water-soluble  
74 exudates and more complex organic compounds resulting from dead cells sloughed off roots [21].  
75 The proportion of photosynthates released in the rhizosphere and composition of the corresponding  
76 rhizodeposits have been shown to vary during the plant's life cycle according to changes in plant

77 physiology during the course of development and the level of symbiotic associations [22]. In addition,  
78 the genetic structure of bacterial and fungal communities was shown to change significantly during  
79 the development of *Medicago truncatula* in both vegetative and reproductive stages and the  
80 intensity of mutualistic symbiotic association with AM fungi and Rhizobia [23]. By extension, changes  
81 in microbial diversity and composition following plant-bioaggressor interactions is often hypothesized  
82 to be based on modifications of the plant chemistry, such as plant exudates [24,25] or root  
83 metabolites [26].

84

85         Microorganisms that are able to penetrate and invade the plant root internal tissues form  
86 the endosphere or root microbiota. The roots of more than 80% of plants are colonized by arbuscular  
87 mycorrhizal fungi (AMF) and thus host symbiosis occurs with few dominant and well-known  
88 microorganisms. On the contrary, inside the Brassicaceae family, plants are believed not to form a  
89 strong symbiosis with few dominant microorganisms but hosts many types of microorganisms,  
90 including Archaea- and Eu-bacteria, fungi, and unicellular eukaryotes, such as algae and amoebae  
91 [27]. So far, only few studies focused on the composition, the dynamics and the ecological functions  
92 of these microorganisms during the plant growth. In contrast to the rhizosphere, the plant roots  
93 feature highly specific microbial communities [28]. The diversity of these endophyte communities is  
94 much lower than that estimated for microbial communities outside the root [10,11]. At the interface  
95 between the rhizosphere and the roots, the rhizoplane is often defined as a specific habitat of the  
96 rhizosphere because it is colonized by microorganisms that are firmly attached to the root surface.  
97 However, selective extraction and analysis of this compartment using culture-independent molecular  
98 methods and high-throughput sequencing are technically difficult and, consequently the role of the  
99 rhizoplane remains poorly understood [28]. Based on the composition of the rhizosphere and root  
100 microbiota, it has been proposed that the plants could assemble their microbiota in two steps, with  
101 the first one involving a rapid recruitment of microorganisms in the vicinity of the root and a second

102 step being their entry inside the root [29]. However, the second step is more complex than the first  
103 one, with each root niche playing a selective role in microbiota assembly [15].

104

105 Even though the composition and recruitment mechanisms of these communities are being  
106 extensively investigated, only few studies dealt with the stability of these assemblies during the plant  
107 growth and under the effect of biotic stresses. Among biotic stresses, soil borne plant pathogens  
108 cause major economic losses in agricultural crops. Most of them are adapted to grow and survive in  
109 bulk soil but can also invade the root tissues to establish parasitic relationships with the plant. Since  
110 soil borne pathogens are already present in the soil before sowing, infections are usually early and  
111 occur during the vegetative stages of plant growth. To infect root tissues, pathogens have to  
112 compete with other microorganisms of the rhizosphere microbiota for available nutrients and  
113 microsites. One of the major roles of the rhizosphere microbial communities could to provide a  
114 frontline defence for plant roots against infection by soil borne pathogens [19]. This is valid not only  
115 for plant but also for animals and humans guts. Some of the mechanisms involved in the activity of  
116 these beneficial rhizosphere microorganisms are well studied and include several direct interactions  
117 with plant pathogens as well as indirect interactions via the plant by stimulating the plant immune  
118 system [30-31]. These mechanisms are well documented, using specific strains, for some  
119 rhizobacteria like *Pseudomonas* sp. and *Bacillus* sp., and for some fungi like *Trichoderma* sp. and non-  
120 pathogenic *Fusarium oxysporum*. However, most of the responsible microbial networks underlying  
121 these defences' mechanisms are currently largely unknown. Recently, some metagenomic  
122 approaches provide us new opportunities to enrich our knowledge about the strong interactions  
123 between telluric pathogens and their living environment.

124

125 In this study, we described the dynamics of the root and rhizosphere (including the  
126 rhizoplane) communities of a Brassicaceae species during its vegetative stages, and we analysed the  
127 effects of a parasitic infection by *Plasmodiophora brassicae* use as a model system, on the

128 composition and dynamics of these microbial communities. This pathogen is responsible for clubroot  
129 disease, a serious disease for many members of the Brassicaceae family. *Plasmodiophora brassicae*  
130 Woronin is a soil borne obligate protist within the class Phytomyxea (plasmodiophorids) of the  
131 protist supergroup Rhizaria [33]. The pathogen life involves three stages: survival in the soil as resting  
132 spores, root hair primary infection and finally secondary cortical infection [34]. This process is  
133 accompanied by the hyperplasia and the hypertrophy of infected roots, resulting in formation of  
134 club-shape galls on the root. The tissue disruption associated with large clubs reduces nutrient and  
135 water transport within the plant, and consequently reduces plant growth and yield. *Brassica rapa*  
136 subsp. *Pekinensis* (Chinese cabbage) was chosen as the plant model of Brassicaceae because the full  
137 *P. brassicae* life cycle was easily achieved under controlled conditions in this species. We specifically  
138 addressed the following questions: (i) what is the dynamics of root and rhizosphere communities of  
139 Chinese cabbage during the vegetative stages of plant growth? (ii) How does *P. brassicae* affect the  
140 composition of bacterial and fungal rhizosphere and root communities at each of its life cycle stages?  
141 and (iii) which microbial species are selected following the infection by *P. brassicae*? To address  
142 these questions, a time-series experiment was conducted under controlled conditions. First, bacterial  
143 and fungal metagenomes of root and rhizosphere communities from non-inoculated (also called  
144 “healthy”) plants were described at successive time points. Then, the trajectories of microbial  
145 communities from healthy and inoculated plants cultivated in the same conditions were compared  
146 over time to analyse the effect of *P. brassicae* on the composition and stability of community  
147 assemblies in *B. rapa* plant roots.

148

## 149 **Materials and methods**

### 150 **Materials**

#### 151 **Soil**

152           The experimental soil used for this study was collected at the INRA experimental site of La  
153 Gruche in Western Brittany (N: 48°08.44', W: 01°47.98'). The topsoil (0-5 cm) was removed and the  
154 layer between -5 and -30 cm was harvested, homogenized, sieved at 4 mm and subsequently stored  
155 in 500 L containers at ambient temperature in the dark until further used. Physical and chemical  
156 properties of the soil were determined at the Arras soil analysis laboratory (F-62000, Arras, France).  
157 These properties were determined as: 13.3% sand, 70.9% silt, 15.8% clay, pH 6.2, 12.0 g.kg<sup>-1</sup> of  
158 organic carbon, 1.2 g.kg<sup>-1</sup> of mineral N and 20.8 g.kg<sup>-1</sup> of organic matter.

## 159 **Pathogen**

160           The selection isolate eH used in this study belongs to the pathotype P1 [35], according to the  
161 host differential set established by [36]. This isolate was kindly provided by J Siemens (University of  
162 Dresden, Germany). It was propagated on Chinese cabbage as root galls, harvested, washed and  
163 stored at -20°C.

## 164 **Plants**

165           Seeds from the highly clubroot susceptible *Brassica rapa* spp. *pekinensis* cv. "Graanat" (ECD5)  
166 were used in this study to conduct the experiments. *B. napus* ssp. *oleifera* cv. "Nevin" (ECD6), *B.*  
167 *napus* ssp. *rapifera* cv. "Wilhelmsburger" (ECD10) and *B. napus* ssp. *oleifera* (Brutor), which  
168 constitute with *B. rapa* spp. *pekinensis* cv. "Graanat" (ECD5) the host differential was used as control  
169 to evaluate the infection success [36].

## 170 **Experimental design**

### 171 **Plant growth assay and inoculation**

172           ECD5 plants were cultivated in pots filled with 400 g of the experimental soil mixed with  
173 sterilized sand in the ratio 2:1. The experiment was conducted under a randomized complete block

174 design using three blocks consisting of three replicates of four plants each. In each block, replicates  
175 were randomly distributed and placed in a greenhouse under the following conditions: 16 hours light  
176 (day) at 22°C and 8 hours dark (night) at 19°C. A mean photosynthetically active photon flux density  
177 of 150  $\mu\text{mol}\cdot\text{m}^{-2}\cdot\text{s}^{-1}$  at plant level during the 16 hours daylight was maintained. Some pots without  
178 plants were designated “bulk soil”.

179 Inoculum was prepared from three galls stored at -20°C as described previously [37]. In brief,  
180 spores were extracted by thawing the frozen galls at room temperature, and then homogenizing in  
181 100 mL of sterilized water at high speed for 2 min. The resulting spore suspension was filtered  
182 through two sieves (250 and 100  $\mu\text{m}$  pore diameters). The spore concentration was determined with  
183 a Malassez cell and adjusted to  $1 \times 10^7$  resting spores. $\text{mL}^{-1}$ . Ten-day-old seedlings were inoculated by  
184 pipetting 1 mL of spore suspension containing  $1 \times 10^7$  spores. $\text{mL}^{-1}$  onto the soil surface at the base of  
185 each seedling. Non-inoculated plants and bulk soil were poured with sterile water. All pots, including  
186 bulk soil controls, were watered periodically every three days from the top with 8 mM Hoagland  
187 solution to maintain a water retention capacity between 70 - 100%.

188

## 189 **Quantification of plant traits**

190 To follow the kinetics of plant growth, four plants per replicate were analyzed at 10 (T1), 17  
191 (T2), 24 (T3), 33 (T4) and 37 (T5) days after sowing (DAS). Standard parameters were recorded:  
192 number of leaves per plant, shoot and root fresh weight, plant leaf areas, plant height and root  
193 length. Statistical analyses were performed using the R software [38]. Data were compared between  
194 healthy and diseased plants using linear models [LMM; function “lmer”, package “lme4”, [39]].  
195 Pairwise comparisons of least square means (LSMeans) were performed using the function “lsmeans”  
196 [package “lsmeans”, [40]] and the false discovery rate (FDR) correction for p-values [41].

## 197 **Symptom development and clubroot severity measurement**



198 Disease severity was assessed in inoculated plants during the vegetative stage of plant  
199 growth at 0 (T1), 7 (T2), 14 (T3), 23 (T4) and 35 (T5) days after inoculation (DAI) with *P. brassicae*,  
200 corresponding to 10, 17, 24, 33 and 45 DAS, respectively. Clubroot severity was recorded using the  
201 scale: 0, no visible swelling; 1, very slight swelling usually confined to lateral roots; 2, moderate  
202 swelling on lateral roots and taproot; 2+, severe clubs on all roots, but some roots remain present;  
203 and 3, no root left, only one big gall. A disease index (DI) was calculated as described by [42]:  $DI =$   
204  $(n_1*25 + n_2*50 + n_3*75 + n_4*100)/N$ , where “ $n_i$ ” is the number of plants in the symptom class “ $i$ ”  
205 and  $N$  is the total number of plants tested. Disease data were analyzed using a likelihood ratio test on  
206 a cumulative link model [40] [CLMM; function “*clmm*”, package “*RVAideMemoire*”, [43]]. Pairwise  
207 comparisons of LSMeans were then computed. To measure the hypertrophy of infected root, taproot  
208 width was also assessed at each date of sampling at 1 cm under the soil surface. Taproot width data  
209 were compared between non-inoculated (or healthy) and inoculated (or diseased) plants using a  
210 linear model [LMM; function “*lmer*”, package “*lme4*”]. Pairwise comparisons of LSMeans [function  
211 “*lsmeans*”, package “*lsmeans*”] and FDR correction for p-values were then performed.

212

## 213 **Sampling of “rhizosphere”, “root” and “bulk soil” compartments**

214

215 Rhizosphere and root compartments from healthy and diseased plants were sampled at 10  
216 (T1), 17 (T2), 24 (T3), 33 (T4) and 45 (T5) DAS. The “rhizosphere compartment” defined as the soil  
217 particles firmly attached to roots was collected by centrifugation of root washings. The “root  
218 compartment” was defined as the root tissues depleted of soil particles and epiphytic bacteria by  
219 sequential washing and sonication treatments and was therefore enriched in root-inhabiting  
220 bacteria.

221

222 Rhizosphere and root samples were collected from planted pots in a soil depth of -1 to -6 cm  
223 from the surface. Roots were separated from non-adhering soil particles, collected in 15 mL Falcon  
224 containing 20 mL sterile water and vortexed for 1 min. Seminal and nodal roots were included in the  
225 analysis. After vortexing, roots were transferred in a sterile Petri dish and subjected to a second  
226 washing treatment with 5 mL sterile water. Double washed roots were transferred in 5 mL sterile  
227 water and sonicated twice for 3 s at 40 Hz to detach microbes living in close association with root  
228 tissues. Roots were transferred in a Petri dish, cut into fragments smaller than 5 mm, ground to a  
229 powder with a pestle in liquid nitrogen-chilled mortar with Fontainebleau sand and stored at -80°C  
230 until further analysis. The soil suspensions collected in the Falcon tubes or in the Petri dishes after  
231 the first, the second washing treatments and the sonicated solution were pooled, centrifuged at  
232 4,000 g for 20 min and the pellet, referred to as the rhizosphere, was frozen in liquid nitrogen and  
233 stored at -80°C until further analysis.

234

235 Soil samples were collected from unplanted pots at T1, T3 and T5 in a soil depth of -1 to -6  
236 cm from the surface. The soils from four pots were pooled, transferred in 10 mL sterile water and  
237 vortexed for 1 min. The soil suspension was centrifuged at 4,000 g for 20 min and the pellet, referred  
238 as the bulk soil, was frozen in liquid nitrogen and stored at -80°C until further analysis.

239

## 240 **DNA extraction and pathogen quantification**

### 241 **Root and soil DNA extraction**

242 The GNS-GII protocol was used for root and DNA extraction [44]. For root samples, five to 150  
243 mg of each root sample were homogenized for 3 x 30 s at 4 m.sec<sup>-1</sup> in a FastPrep<sup>®</sup>-24 (MP-  
244 Biomedicals, NY, USA) in 2 mL of the “lysing matrix E” solution from MpBio containing 100 mM Tris  
245 (pH 8.0), 100 mM EDTA (pH 8.0), 100 mM NaCl, and 2% (wt/vol) sodium dodecyl sulphate. The  
246 samples were incubated for 30 min at 70°C, and then centrifuged at 7,000 g for 1 min at 20°C. To

247 remove proteins from the extracts, 1 mL of the collected supernatant was incubated for 10 min on  
248 ice with 1/10 volume of 3 M potassium acetate (pH 5.5) and centrifuged at 14,000 g for 5 min at 4°C.  
249 Finally, after precipitation with 900 µL of ice-cold isopropanol, the nucleic acids were washed with  
250 70% ice-cold ethanol and DNA was resuspended in 200 µL ultrapure sterile water. DNA was  
251 separated from the residual impurities, particularly humic substances, by centrifuging through two  
252 types of minicolumns. Firstly, aliquots (100 µL) of crude DNA extract were first loaded onto  
253 Microbiospin (Biorad, Hercules, California, USA) columns of PVPP (PolyVinyl PolyPyrrolydone) and  
254 centrifuged at 1,000 g for 2 min at 10°C. Secondly, the eluate was purified with the GeneClean turbo  
255 kit (Q-Biogene, Illkirch, France). DNA concentration and purity were determined with a Nanodrop  
256 (Agilent).

257 The same protocol was used to extract DNA from soil samples except that, before  
258 homogenization in the FastPrep<sup>®</sup>-24, 2 g of each soil sample were mixed with 5 mL of a solution  
259 containing 100 mM Tris (pH 8.0), 100 mM EDTA (pH 8.0), 100 mM NaCl, and 2% (wt/vol) sodium  
260 dodecyl sulphate in a 15 mL “lysing matrix E” Falcon tube from MpBio.

261

## 262 **Measurement of pathogen DNA amount in roots by real-time qPCR**

263 Plant root colonization by *P. brassicae* was also monitored by quantitative PCR. The predicted  
264 18S gene was used to estimate *P. brassicae* DNA amount per ng of total extracted DNA. A portion of  
265 this gene sizing 164 bp was amplified with the primers PbK1F/PbK1R (5'-TTGGGTAATTTGCGCGCCTG-  
266 3'/5'-CAGCGGCAGGTCATTCAACA-3'). All reactions were performed in 20 µL qPCR reaction using 10  
267 µL of SYBR Green Master Mix (Roche), 1 µL of DNA (2.5 ng) and 0.08 µL of each primer (100 µM).  
268 Amplification conditions were as follows: 5 min at 95°C, followed by 45 two-step cycles at 95°C (10s)  
269 and 60°C (40s). Standard curves were constructed using serial dilutions of *P. brassicae* DNA extracted  
270 from resting spores. A linear model [LMM; function “lmer”, package “lme4”] was used to analyze the

271 pathogen DNA quantification data. Pairwise comparisons of LSMeans [function “lsmeans”, package  
272 “lsmeans”] and FDR correction for p-values were then performed.

## 273 **Bacterial and fungal community composition and diversity**

### 274 **Sequencing of 16S and 18S rDNA genes**

275 The structure of microbial communities associated to soil and root samples collected during  
276 the experiments was assessed through amplification and subsequent sequencing of bacterial (16S)  
277 and fungal (18S) rDNA genes. PCR amplification and sequencing were performed at GenoScreen  
278 (Lille, France) using the Illumina Miseq platform to a 2 × 300 bases paired-end version with an  
279 adequate read assembly method. For soil and root DNA extracts, a 420 bp fragment of the V5-V7  
280 region of the bacterial 16S rDNA gene was amplified using the universal bacterial primers 799F\_16S  
281 (5'-AACMGGATTAGATACCKG-3') and 1223R\_16S (5'-CCATTGTAGTACGTGTGTA-3') [45,46]. Before  
282 sequencing, PCR products were purified to eliminate a 760 bp fragment corresponding to plant  
283 mitochondrial DNA amplification. A 530bp fragment of the fungal 18S rDNA that includes the variable  
284 regions V4 (partial) and V5 was also amplified using the primer pair NS22B (5'-  
285 AATTAAGCAGACAAATCACT-3') and SSU0817 (5'-TTAGCATGGAATAATRAATAGGA-3') [47,48].

### 286 **Analysis of MiSeq sequencing data**

287 After reads assembly, sequences were processed with GnS-PIPE bioinformatics platform  
288 developed by GenoSol platform and optimized for amplicons analysis [49,50]. The reads were filtered  
289 and eliminated if they harbored one or more ambiguities (Ns) or an average quality score below 30. A  
290 PERL program was applied to obtain strict dereplication (i.e. clustering of strictly identical  
291 sequences). After this initial quality filtering step, the reads were aligned with INFERNAL alignments  
292 [51] and clustered at 97% sequence similarity into operational taxonomic units (OTU) using another  
293 PERL program. All single-singletons (reads detected only once and not clustered) were then deleted

294 in order to eliminate PCR chimeras and large sequencing errors. These final sequences were used to  
295 produce rarefaction curves. The retained high-quality reads were used for taxonomy-based analysis  
296 of each OTU using similarity approaches against dedicated reference databases from SILVA [52]. The  
297 raw data sets are available on the European Nucleotide Archive database system under the project  
298 accession number PRJEB26948. Root and soil samples accession numbers range from ERS2513216 to  
299 ERS2513353 for 16S and 18S rDNA.

### 300 **Alpha diversity**

301 To compare bacterial or fungal composition among bulk soil, rhizosphere soil and root from  
302 healthy and diseased plants, the richness was characterized by the number of OTUs found in each  
303 sample. As metric of taxonomy diversity, Shannon diversity was also determined using the “vegan”  
304 package in R, version 2.2-1 [53]. Since values were conformed to normality assumptions, two-way  
305 Anova and *post-hoc* Tukey’s HSD test were used to examine pairwise differences between samples  
306 for these measures.

### 307 **Beta diversity**

308 After normalization by sample size, OTU counts without at least a mean of one read per  
309 sample were removed from the analysis. The genera OTU counts were also rarefied to 1,000 counts  
310 per sample and Log2-transformed rarefied values were used to calculate a Bray-Curtis distance  
311 dissimilarity matrix using the function “vegdist” of the R package “Vegan”. The beta diversity distance  
312 matrices were plotted using a bi-dimensional Principal Coordinates Analysis (PCoA) using the  
313 function “plot” of the R package “Vegan”. To quantify the influence of each factor on the beta  
314 diversity, a canonical analysis of principal coordinates (CAP, [54]) followed by a permutation-based  
315 ANOVA (PERMANOVA) was performed using the R package “vegan” according to the method  
316 described by [55].

## 317 **Statistical analysis on phyla counts**

318 To identify phyla enriched in rhizosphere and root microhabitats compared to unplanted soil  
319 and to compare phyla composition between samples collected from healthy and diseased plants, we  
320 employed linear statistics on Relative Abundances (RA) values ( $\log_2 > 5\%$  threshold) using a script  
321 developed from the R package “Limma” [17]. Differentially abundant phyla between two samples  
322 were calculated using moderated t-tests. The resulting p-values were adjusted for multiple  
323 hypotheses testing using the Benjamini-Hochberg (BH) correction.

## 324 **Detection of differentially enriched OTUs**

325 EdgeR is a workflow largely based on the free open-source R language and Bioconductor  
326 software [56]. This workflow was originally used to analyze count-based differential expression of  
327 RNA sequencing as part of transcriptome studies [57] and was recently adapted to metagenomic  
328 data analysis [26]. OTU counts without at least a mean of one read per sample were removed from  
329 the analysis. To normalize the data for each sample OTU count, the trimmed mean of M values  
330 normalization method (TMM) was used according to the method described by [58]. A Log2-  
331 transformation was performed on the normalized data for statistical comparisons. Threshold,  
332 normalization and transformation steps were performed using a custom R script. To identify  
333 differentially abundant genus in bacterial and fungal communities between sampling dates and  
334 treatments (non-inoculated or inoculated) in root or soil samples, EdgeR was used to fit a model with  
335 treatment (non-inoculated or inoculated) \* sampling date (T1 to T5) terms to the count data in each  
336 compartment by using glmFit and glmLRT with tagwise dispersion and to test for significant effects of  
337 each term. EdgeR employs statistical methods supported on negative binomial distribution as a  
338 model for count variability. Data from root and rhizosphere soil were not analyzed together because  
339 composition biases between samples from these two compartments were not eliminated by TMM  
340 normalization. To examine whether having a diverged or conserved communities composition was

341 associated with treatment \* time effect, the model was fitted to subsets of the normalized counts  
342 data and used “contrasts” to identify genera with significant differential abundances in pairwise  
343 comparisons. A likelihood ratio test (LRT) was performed to specify the difference of interest and the  
344 resulting p-values were adjusted for multiple hypotheses testing using the Benjamini-Hochberg (BH)  
345 correction.

## 346 **Results**

347 Chinese cabbage plants were cultivated in a greenhouse for 45 days. Ten days after sowing, the  
348 plants were inoculated or not with *P. brassicae*. The roots and rhizosphere soils from healthy (or non-  
349 inoculated) and diseased (or inoculated) plants were both sampled at 0 (T1), 7 (T2), 14 (T3), 23 (T4)  
350 and 35 (T5) days after inoculation (DAI) with *P. brassicae*, corresponding to 10, 17, 24, 33 and 45 days  
351 after sowing (DAS). Bulk soil was also sampled within non-cultivated plots at T1, T3 and T5. Microbial  
352 composition from each compartment and at each date of sampling was assessed through 16S and  
353 18S high-throughput sequencing. No clubroot symptoms were observed and no *P. brassicae* DNA was  
354 detected in non-inoculated plants.

355

### 356 **Comparison of communities from root, rhizosphere and bulk soils in** 357 **healthy plants: the rhizosphere effect.**

358 In the samples collected at T1, T3 and T5 from healthy plants and bulk soil, the greatest  
359 numbers of bacterial/fungal OTUs were detected in bulk and rhizosphere soils (2,240/1,242 and  
360 2,280/1,220 OTUs on average, respectively) and a significant reduction of richness was observed in  
361 root compartment (530/677 OTUs on average) (S1 and S2 Figs). A significant reduction of bacterial  
362 and fungal diversities in the root samples compared to bulk and rhizosphere soils was also observed  
363 at each sampling date (S1 and S2 Figs). A temporal effect on bacterial richness and diversity was

364 measured but only in the root compartment where the number of OTUs and the Shannon index were  
365 higher at T3. In each compartment, no temporal variations of fungal richness and diversity was  
366 measured.

367

368 When looking at the microbial composition, we found that root bacterial and fungal  
369 communities were clearly distinct from rhizosphere and bulk soil communities at each sampling date  
370 (S3 Fig). A canonical analysis constrained by the variables of interest revealed that for bacterial  
371 communities, the compartment explained 52.5% of the variance ( $p = 0.001$ ; 95% confidence interval  
372 (CI) = 24.5%, 86.7%) and the sampling date explained 5.5% of the variance ( $p = 0.001$ , 95% CI = 4.7%,  
373 6.4%) (S4 Fig). For fungal communities, the compartment explained 29.8% of the variance ( $p = 0.001$ ,  
374 95% CI = 18.7%, 49.4%) and the sampling date 11.8% of the variance ( $p = 0.001$ , 95% CI = 8.7%,  
375 16.2%) (S4 Fig). Consistently, we observed at T5 a clear separation between root microhabitat and  
376 soil samples followed by segregation of the rhizosphere and bulk soil samples. To explain the  
377 variance observed, the significant effect of the sampling date was weaker than the compartment.

378

## 379 **Composition and dynamics of healthy Chinese cabbage rhizosphere** 380 **and root microbiota**

### 381 **In the rhizosphere of healthy plants**

382

383 In the rhizosphere of healthy plants, the most heavily-sequenced bacterial phyla found were  
384 Proteobacteria, Firmicutes, Actinobacteria and Bacteroidetes, with 86% to 90% abundances at each  
385 sampling date between T1 and T5 (Fig 1). Within the rhizosphere-inhabiting Proteobacteria, the  $\alpha$ -  
386 Proteobacteria were over-represented compared to the  $\beta$ -,  $\gamma$ - and  $\delta$ -Proteobacteria (Fig 1). Between  
387 T1 and T5, a significant increase of Proteobacteria ( $\alpha$  and  $\gamma$ ) and a decrease of Firmicutes were  
388 measured while no temporal variation of bulk soil composition at phylum level was observed (data



389 not shown). At T5, the enrichment of members from the Proteobacteria and Bacteroidetes phyla  
390 significantly discriminated rhizosphere from bulk soil samples (data not shown). We tried to narrow  
391 down the bacterial community to those OTUs ( $\geq 97\%$  sequence similarity), which showed a minimum  
392 relative abundance of 0.1% at least in one of the rhizosphere samples. A total of 429 OTUs were  
393 identified in the rhizosphere of healthy plants (S1 Table). At the genus level, OTU1 assigned as  
394 *Bacillus* (Firmicutes) dominated these rhizosphere communities at each sampling date with 12 to  
395 18% relative abundances between T1 and T5. OTU4 (*Sphingomonas*,  $\alpha$ -Proteobacteria), OTU7  
396 (*Pseudolabrys*,  $\alpha$ -Proteobacteria), OTU9 (*Sporosarcina*, Firmicutes), OTU6 (*Bradyrhizobium*,  $\alpha$ -  
397 Proteobacteria), and OTU10 (*Rhodopseudomonas*,  $\alpha$ -Proteobacteria) were also highly represented  
398 (S1 Table). No temporal variation of these dominant OTUs was observed between T1 and T5.  
399 However, several minor OTUs with significant relative abundance variations between two sampling  
400 dates were detected in these bacterial communities (Table 1).

401

402 The fungal rhizosphere communities from healthy plants were largely dominated by Ascomycota,  
403 with 64% to 69% relative abundances between T1 and T4 (Fig 1). Three other phyla, Mucoromycotina  
404 (12% to 16%), Basidiomycota (3% to 8%) and Chytridiomycota (2% to 10%) were also detected but at  
405 lower frequencies. Until T4, the proportions of these four phyla compared to the whole fungal  
406 microbiota were relatively stable. From the 168 fungal OTUs identified with at least a relative  
407 abundance of 0.1% in one of these rhizosphere samples, OTU2 and OTU4, assigned as two  
408 Sordariomycetes, were detected at high frequencies between T1 and T4, but no temporal variations  
409 of these dominant OTUs were observed. At T5, fungi from the Chytridiomycota phylum were  
410 drastically more abundant (47.5%) than at the beginning of the kinetics and a decrease of  
411 Ascomycota (64.6% at T4 to 37.9% at T5) was measured (Fig 1). At this date of sampling, OTU1 and  
412 OTU16, assigned as two Chytridiomycota, were the most abundant OTUs with 18.3 and 16.4%  
413 relative abundances, respectively (S1 Table). Variations of other less dominant OTUs were also  
414 observed between T1 and T5 (Table 1). While the proportion of Chytridiomycota fungi strongly

415 increased in the rhizosphere compartment at T5, their relative abundances remained low in bulk soil  
 416 samples during all the kinetics.

417

418 **Fig 1. Temporal dynamics of the most abundant phyla-subphyla in bacterial (A) and fungal (B)**  
 419 **communities from roots and rhizosphere of healthy plants.** Mean values of abundance (expressed  
 420 in %) were obtained from three replicates per condition and sampling date. Sampling dates refer to  
 421 10 (T1), 17 (T2), 24 (T3), 33 (T4) and 45 (T5) days after sowing. Phyla with relative abundances below  
 422 1% were grouped as “others”. In bacterial communities, the Proteobacteria phylum was divided into  
 423 four subphyla:  $\alpha$ -,  $\beta$ -,  $\gamma$ - and  $\delta$ -Proteobacteria.

424

425 **Table 1. Number of OTUs with significant relative abundance changes between two sampling dates**  
 426 **in the rhizosphere and roots of healthy (non-inoculated) and diseased (inoculated) plants.**

		Rhizosphere		Root	
Down - Up		Bacteria	Fungi	Bacteria	Fungi
<b>NI plants</b>	T1 / T2	0 <sup>a</sup> - 0 <sup>b</sup>	0 - 0	0 - 0	0 - 0
	T1 / T3	0 - 0	0 - 3	8 - 8	1 - 0
	T1 / T4	0 - 0	3 - 0	3 - 9	46 - 5
	T1 / T5	14 - 5	30 - 5	6 - 8	45 - 3
	T2 / T3	0 - 0	0 - 0	3 - 0	1 - 0
	T2 / T4	0 - 1	2 - 0	3 - 2	21 - 2
	T2 / T5	16 - 2	27 - 3	9 - 3	38 - 2
	T3 / T4	0 - 0	4 - 0	1 - 0	13 - 1
	T3 / T5	13 - 1	30 - 0	5 - 5	37 - 1
	T4 / T5	7 - 0	10 - 0	2 - 1	0 - 0
<b>I plants</b>	T1 / T2	0 - 0	0 - 0	0 - 0	10 - 7
	T1 / T3	0 - 0	0 - 0	0 - 0	4 - 1
	T1 / T4	13 - 0	6 - 1	5 - 6	48 - 5
	T1 / T5	46 - 21	27 - 8	13 - 18	40 - 0
	T2 / T3	0 - 0	0 - 0	1 - 0	0 - 0

T2 / T4	17 - 2	3 - 0	5 - 4	0 - 0
T2 / T5	46 - 24	28 - 12	15 - 12	30 - 4
T3 / T4	16 - 0	2 - 0	8 - 1	0 - 0
T3 / T5	42 - 21	31 - 6	21 - 26	36 - 1
T4 / T5	15 - 6	18 - 7	1 - 0	0 - 0

427

428 Number of bacterial and fungal OTUs with significant relative abundance changes (p-values  $\leq 0.05$ )  
 429 between two sampling dates (0 (T1), 7 (T2), 14 (T3), 23 (T4) or 35 (T5) days after inoculation with *P.*  
 430 *brassicae*) in samples from the rhizosphere (RS) and roots (R) of non-inoculated (NI) and inoculated  
 431 (I) Chinese cabbage plants.

432 <sup>a</sup> number of OTUs significantly less abundant at T2 than at T1 in the rhizosphere of NI plants

433 <sup>b</sup> number of OTUs significantly more abundant at T2 than at T1 in the rhizosphere of NI plants

#### 434 **Inside the roots of healthy plants**

435

436 In the roots of healthy plants, bacterial communities were also dominated by Proteobacteria  
 437 (41% to 51% RA between T1 and T5) and Bacteroidetes (21% to 33%) as in the rhizosphere (Fig 1).  
 438 They also contained Actinobacteria (1% to 10%) and Firmicutes (3% to 7%), although to a lesser  
 439 extent than in the rhizosphere samples. In the root samples, the  $\alpha$ - and  $\gamma$ -Proteobacteria were over-  
 440 represented compared to the  $\beta$ - and  $\delta$ -Proteobacteria. Cyanobacteria were also detected. Between  
 441 T1 and T5, more important variations of phylum frequencies occurred in the roots of healthy plants  
 442 than in their rhizosphere (Fig 1). Actinobacteria increased significantly in frequencies while  
 443 Proteobacteria decreased. A total of 202 genera were identified in these communities. The dominant  
 444 OTUs were OTU2 assigned to a *Flavisolibacter* (Bacteroidetes) which relative abundances varied  
 445 between 8% and 17%, OTU3 assigned to an unknown Cyanobacterium, OTU19 (*Devosia*,  $\alpha$ -  
 446 Proteobacteria), OTU12 (*Pseudomonas*,  $\gamma$ -Proteobacteria) and OTU5 (*Flavobacterium*, Bacteroidetes)  
 447 (S1 Table). While the proportion of OTU2 strongly increased in the rhizosphere compartment of

448 healthy plants between T1 and T5, the proportion of OTU19 decreased from 4.2% to 1.0% and no  
449 temporal variations was observed for the other main OTUs. Several other bacterial OTUs with  
450 significant variations in abundances from one date of sampling date to another were also detected in  
451 healthy plant roots (Table 1).

452

453 The root fungal communities were dominated by Ascomycota (85.1%) at T1 and replaced  
454 progressively by fungi from the Chytridiomycota phylum during the kinetics of plant growth. At T5,  
455 OTU1 which was assigned to the Chytridiomycota was detected in the roots of healthy plants at a  
456 very high frequency with a mean of 53% relative abundance (S1 Table). Variations of several minor  
457 OTUs were also observed in the fungal communities of diseased plants during the time-series  
458 experiment (Table 1).

459

460 To conclude, weak fluctuations were measured in the composition of rhizosphere and root  
461 communities of healthy plants before T4, whereas important changes occurred in these communities  
462 between T4 and T5. According to the variations of OTU relative abundances, these changes were first  
463 observed in the bacterial and fungal communities of plant roots and then in the rhizosphere (Table  
464 1).

465

## 466 **Symptom development and clubroot severity**

467 Differences of taproot width between healthy and diseased plants appeared at T3 and increased  
468 drastically between T3 and T5 (Fig 2). Disease index was low at T3 (DI = 16.7%), increased rapidly to  
469 68.5% at T4 and reached a maximum of 86% at the end of the experiment (Fig 2). The amount of *P.*  
470 *brassicae* DNA followed a similar evolution profile (Fig 2). However, although DI increased between  
471 T4 and T5, there were no significant variations of *P. brassicae* DNA amount in roots at these time-  
472 points. Throughout the time of the experiment, no differences of leaf number and leaf area, plant

473 height and shoot biomass were observed between healthy and diseased plants. In contrast, root  
474 length and biomass of inoculated plants decreased significantly but only between T4 and T5 (S2  
475 Table). At the end of the experiment, some galls had become brownish and some mature resting  
476 spores were observed in gall tissues. According to these results, the duration of the life cycle of *P.*  
477 *brassicae* infection in Chinese cabbage was approximately 35 days in our experimental conditions.  
478 The root hair infection and the beginning of the cortical infection stages occurred before 14 DAI, and  
479 clubroots formed gradually between 14 and 35 DAI.

480 **Fig 2. Clubroot disease development.** The clubroot development was measured in greenhouse  
481 conditions on Chinese cabbage roots over successive sampling at 0 (T1), 7 (T2), 14 (T3), 23 (T4) and  
482 35 (T5) days after inoculation (DAI) by *P. brassicae*. **A)** Taproot width comparison at 1 cm under the  
483 soil surface between non-inoculated (NI) and inoculated (I) plants at each date of sampling. Each  
484 histogram bar represents the mean of three replicates of four plants. Dot and stars indicate  
485 statistically different LSM means (.:  $P \leq 0.1$ , \*:  $P \leq 0.05$ , \*\*:  $P \leq 0.01$ , \*\*\*:  $P \leq 0.001$ ). **B)** Disease index  
486 (DI) and pathogen DNA amount (per ng of total DNA) in roots of I plants at each date of sampling. DI  
487 indices were represented by the histogram bars and pathogen DNA amount by the black lines. Each  
488 dot or histogram bar represents the mean of three replicates of four pooled plants. Capital and  
489 lowercase letters indicate statistical differences ( $p$ -values  $\leq 0.05$ ) between sampling dates for DI and  
490 pathogen DNA amounts, respectively.

491

## 492 **Effect of *P. brassicae* on the rhizosphere and root microbiota of**

### 493 **Chinese cabbage**

#### 494 **In the rhizosphere of diseased plants compared to healthy plants**

495

496 In the rhizosphere compartment, no significant variation of bacterial richness and diversities  
497 was measured between healthy and diseased plants whatever the sampling date (T1 to T5) (S5 Fig).  
498 The same results were observed in fungal communities except that a reduction of diversity occurred  
499 in the rhizosphere of diseased plants at the end of the experiment at T5 (S6 Fig). In bacterial  
500 communities, the sampling date explained 21.2% of the overall variance of the data ( $p = 0.001$ , 95%  
501 CI = 19.5%, 24.3%) and the inoculation condition (I vs NI) 4.4% of this variance. This proportion of the  
502 variation, albeit small, was found significant ( $p = 0.02$ , 95% CI = 3.3%, 5.3%). The microbial dynamics  
503 of healthy and diseased plant communities clearly diverged from T3 to T5 as visualized in PCoA (Fig  
504 3). At T4, there is no variation of bacterial phyla\_subphyla relative abundances between healthy and  
505 diseased plants (Fig 4), but two OTUs (OTU35 and OTU188) assigned to two genera from the  $\alpha$ -  
506 Proteobacteria phylum (*Sphingopyxis* and *Rhodobacter*, respectively) and two non-assigned  $\beta$ -  
507 Proteobacteria (OTU54 and OTU151) became more abundant in the rhizosphere of diseased than  
508 healthy plants (Fig 5). At T5, Proteobacteria ( $\alpha$ ,  $\beta$  and  $\gamma$ ) and Bacteroidetes were consistently more  
509 abundant in the rhizosphere of diseased than healthy plants, while both Firmicutes and  
510 Acidobacteria were less abundant (Fig 4). At this sampling date, 20 OTUs belonging mainly to the  
511 Proteobacteria, Bacteroidetes and Firmicutes phyla were significantly more abundant in inoculated  
512 than in non-inoculated plant samples and 8 less abundant (Fig 5). Among these 28 rhizospheric OTUs,  
513 the more frequent ones were OTU1 (*Bacillus*) that decreased between T1 and T5 in the rhizosphere  
514 of all plants but more drastically in diseased plants especially at T5, and OTU5 (*Flavobacterium*),  
515 OTU14 (*Dokdonella*), OTU17 (*Pseudomonas*), OTU35 (*Sphingopyxis*), OTU54 (unknown  $\beta$ -  
516 Proteobacteria) which were all significantly more abundant in inoculated than non-inoculated  
517 samples at T5 (Fig 6). In fungal communities, the sampling date explained a higher proportion of the  
518 variance than in bacterial communities (35%,  $p = 0.001$ , 95% CI = 26.1%, 49%), while the inoculation  
519 condition (inoculated vs non-inoculated) had no significant effect (3.9%,  $p = 0.077$ , 95% CI = 2.8%,  
520 5.6%). Until T4, no variation of fungal phylum frequencies was observed (Fig 4). At T5, while  
521 Ascomycota, Basidiomycota and Mucoromycotina were less abundant in the rhizosphere of diseased

522 than healthy plants, no significant variation of Chytridiomycota was observed (Fig 4). However, the  
523 major OTU (OTU1) assigned to the Chytridiomycota phylum significantly increased in diseased plant,  
524 while four minor OTUs also varied: higher relative abundances for OTU55 and OTU60 but lower for  
525 OTU11 and OTU20 in diseased than healthy plant samples at T5 (Fig 7). Higher changes of OTU  
526 relative abundances occurred in diseased than healthy plant rhizosphere communities during the  
527 time-series experiment (Table 1).

528

529 **Fig 3. Unconstrained Principal Coordinate Analysis (PcoA) of bacterial and fungal communities from**  
530 **non-inoculated (NI) and inoculated (I) plants.** The variances explained by PCoA axes are given in  
531 parenthesis. Compartment refers to rhizosphere soil and roots. Sampling date refers to 0 (T1), 7 (T2),  
532 14 (T3), 23 (T4) and 35 (T5) days after inoculation (DAI) with *P. brassicae*, corresponding to plus,  
533 crosses, circles, triangles and squares, respectively. Condition refers to non-inoculated (NI) and  
534 inoculated (I) plants, represented by green and red colours, respectively.

535

536 **Fig 4. Relative abundances of the most abundant phyla-subphyla in bacterial (A) and fungal (B)**  
537 **communities from root (R) and rhizosphere (RS) compartments.** Mean values of abundance  
538 (expressed in %) were obtained from three replicates per condition and sampling date. Condition  
539 refers to non-inoculated (NI) and inoculated (I) plants. Sampling date refers to 0 (T1), 7 (T2), 14 (T3),  
540 23 (T4) and 35 (T5) days after inoculation (DAI) by *P. brassicae*. Phyla with relative abundances below  
541 1% were grouped as “others”. At each sampling date, significant ( $p$ -values  $\leq 0.05$ ) and non-significant  
542 differences between NI and I plants are indicated by stars and “ns”, respectively. In bacterial  
543 communities, the Proteobacteria phylum was divided into four subphyla:  $\alpha$ -,  $\beta$ -,  $\gamma$ - and  $\delta$ -  
544 Proteobacteria.

545

546 **Fig 5. Bacterial OTU relative abundances in the root and rhizosphere microbiota of non-inoculated**  
547 **(NI) and inoculated (I) plants.** Bacterial OTUs that significantly differed in their relative abundances

548 (expressed in %) in the root and rhizosphere samples between I and NI plants are represented.  
549 Differences were only observed at T4 and T5 in both compartments. Each histogram bar represents  
550 the mean RA ( $\pm$  SEM) of three replicates. Only significant differences ( $p$ -values  $\leq 0.05$ ) between I and  
551 NI plants (represented by white and black bars, respectively) are shown, hence at T4 and T5 in both  
552 compartments. Framed numbers indicate the number of OTUs with significant different frequencies  
553 between I and NI plants.

554

555 **Fig 6. Temporal dynamics of bacterial OTU relative abundances in the bacterial rhizosphere**  
556 **microbiota of non-inoculated (NI) and inoculated (I) plants.** Relative abundances (expressed in %) of  
557 the most abundant OTUs in rhizosphere (R) at each date of sampling are represented. Sampling date  
558 refers to 0 (T1), 7 (T2), 14 (T3), 23 (T4) and 35 (T5) days after inoculation (DAI) with *P. brassicae*. Each  
559 dot represents the mean value of relative abundance ( $\pm$  SEM) of three replicates. Stars indicate  
560 significant differences ( $p$ -values  $\leq 0.05$ ) between NI and I plants (represented respectively by black  
561 and grey lines) at each sampling date.

562

563 **Fig 7. Fungal OTU relative abundances in the rhizosphere microbiota of non-inoculated (NI) and**  
564 **inoculated (I) plants.** Fungal OTUs that significantly differ in their relative abundances (expressed in  
565 %) in rhizosphere samples (RS) between I and NI plants at T5 are represented. Differences were only  
566 observed at T5 in the rhizosphere compartment. Each histogram bar represents the mean relative  
567 abundances ( $\pm$  SEM) of three replicates. Only significant differences ( $p$ -values  $\leq 0.05$ ) between I and  
568 NI plants (represented by white and black bars, respectively) are shown, hence at T5 in the  
569 rhizosphere compartment. Framed numbers indicate the number of OTUs with significant different  
570 frequencies between I and NI plants.

571

572 **Inside the roots of diseased plants compared to healthy plants**

573



574 In the root compartment, no clear significant differences of bacterial and fungal richness and  
575 diversity of communities from healthy and diseased plants were found at each date of sampling (S5  
576 and S6 Figs). In bacterial communities, the sampling date explained 24.4% of the overall data  
577 variance ( $p = 0.001$ , 95% CI = 20.9%, 28.1%) and the inoculation condition (inoculated vs non-  
578 inoculated) 6.2% of this variance ( $p = 0.002$ , 95% CI = 4.4%, 8.2%). No significant differences in  
579 community composition between inoculated and non-inoculated root samples were observed until  
580 T4 when one bacterial OTU (OTU2) assigned to the *Flavisolibacter* genus decreased drastically in  
581 relative abundances, while six minor OTUs (OTU54, OTU151, OTU122, OTU150 and OTU422 and  
582 OTU440) were slightly more abundant in inoculated than non-inoculated samples (Fig 5). At T5,  
583 Actinobacteria were less abundant in the roots of diseased than healthy plants but  $\beta$ -Proteobacteria  
584 were more abundant at the phyla-subphyla level (Fig 4). We observed significant differences in  
585 relative abundances of 28 OTUs between inoculated and non-inoculated root samples. Among these  
586 28 OTUs, OTU2 (*Flavisolibacter*), OTU21 (*Streptomyces*) and OTU44 (*Pseudomonas*), were the main  
587 OTUs which relative abundances had decreased in diseased plants on one hand (Fig 8). On the other  
588 hand, the main OTUs which frequencies increased in inoculated vs non-inoculated plants were  
589 OTU17 (*Pseudomonas*) but also the two non-assigned  $\beta$ -Proteobacteria OTU54 and OTU62 (Fig 8).  
590 Regarding fungal communities, the date of sampling accounted for a higher proportion of the  
591 variance than in bacterial communities (36.6%,  $p = 0.001$ , 95% CI = 26.2%, 52.9%), while the  
592 condition (inoculated vs non-inoculated) had no significant effect (2.7%,  $p = 0.55$ , 95% CI = 1.7%,  
593 3.9%) as in the rhizosphere. At each date of sampling, there was no difference in fungal phylum (Fig  
594 4) and OTUs frequencies between diseased and healthy root samples. However, changes of OTU  
595 relative abundances occurred in root communities of healthy and diseased plants during the time-  
596 series experiment (Table 1).

597

598 **Fig 8. Temporal dynamics of bacterial OTU relative abundances in the root microbiota of non-**  
599 **inoculated (NI) and inoculated (I) plants.** Relative abundances (expressed in %) of the most

600 abundant OTUs in root (R) at each date of sampling are represented. Date of sampling refers to 0  
601 (T1), 7 (T2), 14 (T3), 23 (T4) and 35 (T5) days after inoculation (DAI) with *P. brassicae*. Each dot  
602 represents the mean value of relative abundance ( $\pm$  SEM) of three replicates. Stars indicate  
603 significant differences ( $p$ -values  $\leq 0.05$ ) between inoculated (I) and non-inoculated (NI) plants  
604 (represented by black and grey lines, respectively) at each sampling date.

605

## 606 **Discussion**

607

608 In our study, the stability of assembled root and rhizosphere communities of Chinese  
609 cabbage was investigated by a time-series experiment, during the plant growth and under the effect  
610 of the parasitic invasion by *P. brassicae*. During the plant growth, for healthy plants, most of  
611 Ascomycota fungi previously recruited by the plant were replaced, mainly in the root compartment,  
612 by a Chytridiomycota fungus. The root and rhizosphere-associated community assemblies were also  
613 strongly modified by *P. brassicae* infection during the secondary cortical infection stage of clubroot  
614 disease.

615

### 616 **A weak but significant rhizosphere effect**

617

618 Clearly, the communities that assembled in the rhizosphere and bulk soils of healthy plants  
619 were very different from the communities found in the roots. These results are consistent with  
620 earlier findings on other plant species [2,10,15,59,60]. We found a significant “rhizosphere effect”.  
621 Indeed, the alpha diversity analysis showed that the microbiota diversities of the bulk and  
622 rhizosphere soils were not distinct from each other. These observations are similar to the findings of  
623 several authors in *Arabidopsis thaliana* who reported the resemblance of bacterial communities  
624 between rhizosphere and bulk soil samples in multiple soil types [2,10]. At each sampling date, bulk

625 soil and rhizosphere compartments shared a large proportion of OTUs. However, the enrichment of  
626 OTUs assigned to the Proteobacteria and Bacteroidetes bacterial phyla, but also to the  
627 Chytridiomycota fungal phylum, significantly discriminated rhizosphere from bulk soil samples at the  
628 end of the experiment.

629

## 630 **The structure of microbial communities associated with the** 631 **rhizosphere and roots of healthy plants evolved over time**

632

633 Roots and rhizosphere of healthy plants were preferentially colonized by Proteobacteria and  
634 Bacteroidetes bacterial phyla. Rhizosphere bacterial communities also contained Actinobacteria and  
635 Firmicutes but to a higher extent than in the roots. This result was expected because Proteobacteria,  
636 Bacteroidetes and Actinobacteria phyla were also highly abundant in the rhizosphere soil of many  
637 *Brassicaceae* species like *A. thaliana* [2] and *B. napus* [61-63], with the exception of Bacteroidetes  
638 being present at low frequencies in the rhizosphere of *B. napus* cultivated in a Podzol [61] and in a  
639 soil collected from an organically managed field [63]. Furthermore, higher frequencies of Firmicutes  
640 were observed in rhizosphere communities of Chinese cabbage than in other *Brassicaceae* species.  
641 Actinobacteria were detected at lower frequencies in the roots of Chinese cabbage than in the roots  
642 of *A. thaliana* [2,10] and *B. napus* [61,62,64]. As in the roots of all *Brassicaceae*, Cyanobacteria were  
643 also abundant in the root of Chinese cabbage.

644

## 645 **A fungus belonging to the Chytridiomycota phylum became** 646 **dominant in the roots and rhizosphere of non-inoculated plants**

647

648           The variations of fungal OTU frequencies in the communities of healthy plants were observed  
649   mainly at the two last sampling dates. The main changes in fungal communities concerned the  
650   relative abundances of an unknown Chytridiomycota which increased drastically at the end of the  
651   experiment in the two plant compartments, but especially in roots. This fungus replaced Ascomycota  
652   fungi that were previously dominant. In contrast to bacterial 16S sequences, fewer fungal 18S  
653   sequences were available to use in taxonomic assignment. However, [65] described the fungal  
654   rhizosphere microbiota succession of *B. rapa* plants in compost over three plant generations by  
655   sequencing of ITS regions. From the second generation, the Chytridiomycota fungus assigned as  
656   *Olpidium brassicae* became dominant in the rhizosphere fungal communities. The organism in our  
657   samples could be *O. brassicae* or a close relative, but ultimately this would require confirmation by  
658   culturing or more extensive sequencing. This fungus is considered as a soilborne obligate parasite  
659   that invades *Brassica* rhizosphere, infects roots and reduces production of pods and seeds [66,67]. Its  
660   resting spores can remain dormant in the soil for up to 20 years before infecting roots. However, no  
661   symptom was observed on non-inoculated plant roots in our study. For a non-mycorrhized plant, we  
662   wondered whether such an endophytic fungus could play a role in plant nutrition or protection  
663   against biotic or abiotic stresses as it was observed with *Colletotrichum* spp. [68].

664

## 665   **Clubroot disease altered microbial community structure from the** 666   **Chinese cabbage roots, then from its rhizosphere**

667

668           To analyse how the soil borne pathogen affects bacterial and fungal root communities,  
669   Chinese cabbage seedlings were inoculated by *P. brassicae* resting spores ten days after sowing. Non-  
670   inoculated and inoculated plants were cultivated in controlled conditions for 45 days after sowing.  
671   The bacterial and fungal metagenomes from the roots and rhizosphere of healthy and diseased plants  
672   were compared at several sampling dates after inoculation. We demonstrated that the invasion by a

673 soilborne parasite changed root and rhizosphere microbial communities already assembled from the  
674 soil. Such results about the impact of a soilborne pathogen on the indigenous plant-associated  
675 microbiome was also described for *Rhizoctonia solani* on the lettuce microbiome [69] and for  
676 *Ralstonia solanacearum* on the tomato rhizosphere microbiota [70].

677

678         After inoculation, resting spores of *P. brassicae* released zoospores, which invaded the plant  
679 rhizosphere, reached the surface of the root hair and penetrated through the cell wall inside root  
680 hairs to form primary plasmodia. After nuclear divisions, the primary plasmodia differentiated into  
681 zoosporangia and secondary zoospores were formed in each zoosporangium to be released into the  
682 rhizosphere soil [34]. During this primary infection stage, *P. brassicae* was not detected in roots by  
683 quantitative PCR indicating that the amount of protist was very low. The interactions between the  
684 primary and secondary zoospores and the plant microbiota by direct or indirect mechanisms did not  
685 result in detectable changes in bacterial and fungal communities, neither in the roots, nor in the  
686 rhizosphere. After being released, the secondary zoospores penetrate the taproot cortical tissues.  
687 Inside invaded taproot cells, the pathogen develops into secondary plasmodia which are associated  
688 to cellular hypertrophy, followed by gall formation in the tissues [34]. This secondary infection stage  
689 was localized inside the roots. During this cortical infection, the amount of *P. brassicae* increased  
690 drastically and multiple direct interactions between the protist and the endosphere communities  
691 could occur.

692

693         We demonstrated that when *P. brassicae* developed inside the roots during its secondary  
694 infection stage, it strongly modified the endophytic bacterial communities and lightly the fungal  
695 communities. Then, probably as a consequence of the disturbances caused by the interactions  
696 between *P. brassicae* and the endophytic communities inside the roots, shifts in rhizosphere  
697 communities of diseased plants occurred only at the last date of sampling. Changes in plant  
698 microbiota probably occurred by direct microbe-microbe interactions, mainly in the root

699 compartment and then by direct microbial exchanging between the two compartments. However,  
700 changes in microbial composition following plant-parasite interactions are often hypothesized to be  
701 based on some modifications of the plant chemistry. Salicylic Acid (SA) and Jasmonic Acid (JA) are  
702 important hormonal regulators of the plant immune signalling network in which it is commonly  
703 accepted that SA is effective against biotrophic and JA against necrotrophic pathogens. However, *P.*  
704 *brassicae* is a biotrophic parasite and both SA and JA signalling pathways could play a role in partial  
705 inhibition of clubroot development in compatible interactions between *A. thaliana* and *P. brassicae*  
706 [71]. The defence-related phytohormones SA and JA are also known to important modulators of  
707 microbiota assembly of *A. thaliana* [72,73]. The accumulation of SA and/or JA or both in plant roots  
708 in response to *P. brassicae* infection could lead to modify the composition of plant rhizodeposits and  
709 to stimulate specific microbiota in the roots and rhizosphere.

710

711         These direct microbe-microbe or indirect microbe-plant interactions could drive the selection  
712 of a plant protective microbiome. In few situations, the competitive interaction between soil borne  
713 pathogens and root microbiota for available nutrients and microsites could lead to a strong  
714 restriction of the pathogen by the activities of specific microorganisms. These situations were already  
715 described in suppressive soils for soil borne [74] and foliar parasites [75]. A sequence of events taking  
716 place in the rhizosphere of sugar beet seedlings growing in a disease suppressive soil infected by *R.*  
717 *solani* was proposed as a model [74]. The fungus may induce, directly or indirectly via the plant,  
718 stress responses in the rhizosphere microbiome by the production of oxalic and phenylacetic acid  
719 and lead to shifts in microbiome composition by the activation of Oxalobacteraceae,  
720 Burkholderiaceae, Sphingobacteriaceae and Sphingomonadaceae families present in the suppressive  
721 rhizosphere microbiome. This stress in turn could trigger a response in these bacterial families,  
722 leading to the activation of antagonistic traits that restrict pathogen infection [74].

723

724 In light of our results, we also propose a model (Fig 9) in which *P. brassicae* during the first  
725 step of its life cycle crosses the plant rhizosphere and infect the root hair without inducing changes in  
726 microbiota composition as a consequence of plant metabolism modification. Then, the parasite  
727 penetrates inside the roots during the second step of its life cycle and induces due to gall growth  
728 strong modifications of the root microbiota. This invasion leads to modification of plant metabolites  
729 and root exudates, but also to induction of the plant immune system. As consequences of these  
730 trophic and defence modifications, we observed the selection in the root microbiota of specific  
731 microorganisms that could (i) use new metabolites, (ii) produce a signal triggering defense responses  
732 in plants and (iii) activate, directly or indirectly, other microorganisms in the root and rhizosphere  
733 microbiota to control the protist. Future studies will focus on investigating these hypotheses by,  
734 among others, selecting other soils and plant genotypes to promote the mechanisms that lead to the  
735 restriction of parasitic infection. We also want to develop more functional analysis of the plant-  
736 microbiota interactions to identify the underlying mechanisms.

737

738 The importance of microbiome for the functioning of plant has been widely recognized.  
739 Understanding the complex interactions between the pathogen or more generally biotic stress, the  
740 plant and its rhizosphere microbiome network are also key elements in shaping a plant-protective  
741 microbiome to improve the efficacies of biocontrol agents and partially resistant plants in controlling  
742 soil borne plant diseases. By this, plant microbiome is expected to have an important impact in  
743 biotechnology and will be a key point for the next Green Revolution as a harbinger to draw a new  
744 model for sustainable agriculture.

745

746 Fig 9. Model illustrating the proposed sequence of events (A to C) taking place in the roots and  
747 rhizosphere of Chinese cabbage plant during invasion by *P. brassicae*. Depicted are the changes in  
748 microbial community composition in the two compartments as consequences of potential changes in  
749 root exudation and plant defense reactions.

## 750 Acknowledgment

751

752 The authors thank Christine Lariagon and Yannick Lucas for their technical assistance. They also thank  
753 Hector Mougél for helping to design to Fig 9 and Maxime Hervé for his advises on statistical analyses.  
754 The authors would like to thank the BrACySol biological resource centre (INRA, IGEPPloudaniel,  
755 France) for providing the seeds used in this study. This work has benefited from the involvement of  
756 bioinformatics service of the GenoSol platform from the INRA (French National Institute for  
757 Agronomic Research) of Dijon.

758

## 759 References

760

761

762 1. Berendsen RL, Pieterse CM, Bakker PA. The rhizosphere microbiome and plant health. Trends  
763 Plant Sci. 2012; 17:478–486. doi:10.1016/j.tplants.2012.04.001.

764

765 2. Lundberg DS, Lebeis SL, Paredes SH, Yourstone S, Gehring J, Malfatti S, et al. Defining the  
766 core *Arabidopsis thaliana* root microbiome. Nature. 2012;488(7409): 86–90.  
767 doi:10.1038/nature11237.

768

769 3. Vorholt JA. Microbial life in the phyllosphere. Nat Rev Microbiol. 2012;10(12): 828–840.  
770 doi:10.1038/nrmicro2910.

771

772 4. Vacher C, Hampe A, Porté AJ, Sauer U, Compant S, Morris CE. The phyllosphere: microbial  
773 jungle at the plant-climate interface. Annu Rev Ecol Evol Syst. 2016;47: 1–24.  
774 doi:10.1146/annurev-ecolsys-121415-032238.

775

776 5. Barret M, Briand M, Bonneau S, Prévieux A, Valière S, Bouchez O, et al. Emergence shape  
777 the structure of the seed microbiota. Appl Environ Microbiol 2015;81: 1257–66.  
778 doi:10.1128/AEM.03722-14.

779

780 6. Schiltz S, Gaillard I, Pawlicki-Jullian N, Thiombiano B, Mesnard F, Gontier E. A review: what is  
781 the spermosphere and how can it be studied? J Appl Microbiol. 2015;119: 1467–81.  
782 doi:10.1111/jam.12946.

783

784 7. Berg G, Rybakova D, Grube M, Köberl M. The plant microbiome explored: implications for  
785 experimental botany. J Exp Bot. 2016; 67: 995–1002. doi:10.1093/jxb/erv466.

786

787 8. Bakker PAHM, Berendsen RL, Doornbos RF, Wintermans PCA, Pieterse CMJ. The rhizosphere  
788 revisited: root microbiomics. Front Plant Sci. 2013;4: 165. doi:10.3389/fpls.2013.00165.

789



- 790 9. Mendes R, Garbeva P, Raaijmakers JM. The rhizosphere microbiome: significance of plant  
791 beneficial, plant pathogenic, and human pathogenic microorganisms. FEMS Microbiol Rev.  
792 2013;37: 634–663. doi:10.1111/1574-6976.12028.  
793
- 794 10. Bulgarelli D, Rott M, Schlaeppi K, Ver Loren van Themaat E, Ahmadinejad N, et al. Revealing  
795 structure and assembly cues for *Arabidopsis* root-inhabiting bacterial microbiota. Nature.  
796 2012;488: 91–95. doi:10.1038/nature11336.  
797
- 798 11. Schlaeppi K, Dombrowski N, Garrido-Oter R, Ver Loren van Themaat E, Schulze-Lefert P.  
799 Quantitative divergence of the bacterial root microbiota in *Arabidopsis thaliana* relatives.  
800 Proc Natl Acad Sci USA. 2014;111: 585–592. doi:10.1073/pnas.1321597111.  
801
- 802 12. Lennon JT, Jones SE. Microbial seed banks: the ecological and evolutionary implications of  
803 dormancy. Nat Rev Microbiol. 2011;9: 119–130. doi:10.1038/nrmicro2504.  
804
- 805 13. Hartmann A, Rothballer M, Schmid M. Lorenz Hiltner, a pioneer in rhizosphere. Microbial  
806 ecology and soil bacteriology research. Plant Soil. 2008;312: 7–14. doi:10.1007/s11104-007-  
807 9514-z.  
808
- 809 14. Hartmann A, Schmid M, van Tuinen D, Berg G. Plant-driven selection of microbes. Plant Soil.  
810 2009;321: 235–257. doi:10.1007/s11104-008-9814-y.  
811
- 812 15. Edwards J, Johnson C, Santos-Medellín C, Lurie E, Podishetty NK, Bhatnagar S, et al.  
813 Structure, variation, and assembly of the root-associated microbiomes of rice. Proc Natl Acad  
814 Sci USA. 2015;112: E911–E920. doi :10.1073/pnas.1414592112.  
815
- 816 16. Ranjard L, Dequiedt S, Chemidlin Prévost-Bouré N, Thioulouse J, Saby NP, et al. Turnover of  
817 soil bacterial diversity driven by wide-scale environmental heterogeneity. Nature Commun.  
818 2013;4: 1434. doi:10.1038/ncomms2431.  
819
- 820 17. Bulgarelli D, Garido-Oter R, Münch PC, Weiman A, Dröge J, Pan Y, et al. Structure and  
821 function of the bacterial root microbiota in wild and domesticated barley. Cell Host Microbe.  
822 2015;17: 392–403. doi:10.1016/j.chom.2015.01.011.  
823
- 824 18. Mahoney AK, Yin C, Hulbert SH. Community structure, species variation, and potential  
825 functions of rhizosphere-associated bacteria of different winter wheat (*Triticum aestivum*)  
826 cultivars. Front Plant Sci. 2017;8: 132. doi:10.3389/fpls.2017.00132.  
827
- 828 19. Cook RJ, Thomashow LS, Weller DM, Fujimoto D, Mazzola M, Bangera G, et al. Molecular  
829 mechanisms of defense by rhizobacteria against root disease. Proc Natl Acad Sci USA.  
830 1995;92: 4197–4201. doi :10.1073/pnas.92.10.4197.  
831
- 832 20. Marilley J, Aragno M. Phylogenetic diversity of bacterial communities differing in degree of  
833 proximity of *Lolium perenne* and *Trifolium repens* roots. Appl Soil Ecol. 1999;13: 127–136.  
834 doi :10.1016/S0929-1393(99)00028-1.  
835
- 836 21. Bowen GD, Rovira AD. The rhizosphere: the hidden half of the hidden half. In: Waisel Y, Eshel  
837 A, Kafkafi U, eds. Plant roots: the hidden half. New York, NY, USA: Marcel Dekker. 1991;641–  
838 670.  
839

- 840 22. Gransee A, Wittenmayer L. Qualitative and quantitative analysis of water-soluble root  
841 exudates in relation to plant species and development. *J. Plant Nutr. Soil Sci.* 2000;163: 381–  
842 385. doi :10.1002/1522-2624(200008)163:4<381::AID-JPLN381>3.0.CO;2-7.  
843
- 844 23. Mougél C, Offre P, Ranjard L, Corberand T, Gamalero E, Robin C, Lemanceau P. Dynamic of  
845 the genetic structure of bacterial and fungal communities at different development stages of  
846 *Medicago truncatula* Gaertn. cv. Jemalong J5. *New Phytol.* 2006;170: 165-175.  
847 doi:10.1111/j.1469-8137.2006.01650.x.  
848
- 849 24. Kim B, Song GC, Ryu C-M. Root exudation by aphid leaf infestation recruits root-associated  
850 *Paenibacillus* spp. to lead plant insect susceptibility. *J. Microbiol. Biotechnol.* 2016;26: 549–  
851 557. doi:10.4014/jmb.1511.11058.  
852
- 853 25. Kong HG, Kim BK, Song GC, Lee S, Ryu C-M. Aboveground whitefly infestation-mediated  
854 reshaping of the root microbiota. *Front. Microbiol.* 2016;7: 1314.  
855 doi:10.3389/fmicb.2016.01314.  
856
- 857 26. Ourry M, Lebreton L, Chaminade V, Guillerm-Erckelboudt A-Y, Hervé M, Linglin J, et al.  
858 Influence of belowground herbivory on the dynamics of root and rhizosphere microbial  
859 communities. *Front Ecol Evol.* 2018;6(91). doi.org/10.3389/fevo.2018.00091.  
860
- 861 27. Hardoim PR, van Overbeek LS, Berg G, Pirttilä AM, Compant S, Campisano A, et al. The  
862 hidden world within plants: ecological and evolutionary considerations for defining  
863 functioning of microbial endophytes. *Microbiol Mol Biol Rev.* 2015;79: 293–320.  
864 doi:10.1128/MMBR.00050-14.  
865
- 866 28. Vandenkoornhuyse P, Quaiser A, Duhamel M, Le Van A, Dufresne A. The importance of the  
867 microbiome of the plant holobiont. *New Phytol.* 2015;206: 1196–206.  
868 doi:10.1111/nph.13312.  
869
- 870 29. Bulgarelli D, Schlaeppi K, Spaepen S, Ver Loren van Thermaat E, Schulze-Lefert P. Structure  
871 and functions of the bacterial microbiota of plants. *Annu Rev Plant Biol.* 2013;64: 807–83.  
872 doi:10.1146/annurev-arplant-050312-120106.  
873
- 874 30. Weller DM, Raaijmakers JM, Gardener BB, Thomashow LS. Microbial populations responsible  
875 for specific soil suppressiveness to plant pathogens. *Annu Rev Phytopathol.* 2002;40: 309–  
876 348. doi: 10.1146/annurev.phyto.40.030402.110010.  
877
- 878 31. Lugtenberg B, Kamilova F. Plant-growth promoting rhizobacteria. *Annu Rev Microbiol.*  
879 2009;63: 541– 556. doi:10.1146/annurev.micro.62.081307.162918.  
880
- 881 32. Raaijmakers JM, Paulitz TC, Steinberg C, Alabouvette C, Moëgne-Loccoz Y. The rhizosphere: a  
882 playground and battlefield for soilborne pathogens and beneficial microorganisms. *Plant Soil.*  
883 2009;321: 341–361. doi:10.1007/s11104-008-9568-6.  
884
- 885 33. Hwang S-F, Strelkov SE, Feng JIE, Gossen BD, Howard RJ. *Plasmodiophora brassicae*: a review  
886 of an emerging pathogen of the Canadian canola (*Brassica napus*) crop. *Mol Plant Pathol.*  
887 2012;13: 105–113. doi:10.1111/J.1364-3703.2011.00729.x.  
888
- 889 34. Kageyama K, Asano T. Life Cycle of *Plasmodiophora brassicae*. *J Plant Growth Regul.* 2009;28:  
890 203–211. doi:10.1007/s00344-009-9101-z.

- 891  
892 **35.** Föhling M, Graf H, Siemens J. Pathotype separation of *Plasmodiophora brassicae* by the host  
893 plant. J Phytopathol. 2003;151: 425–430. doi:10.1046/j.1439-0434.2003.00744.x.  
894  
895 **36.** Somé A, Manzanares MJ, Laurens F, Baron F, Thomas G, Rouxel F. Variation for virulence on  
896 *Brassica napus* L. amongst *Plasmodiophora brassicae* collections from France and derived  
897 single-spore isolates. Plant Pathol. 1996;45: 432–439. doi:10.1046/j.1365-3059.1996.d01-  
898 155.x.  
899  
900 **37.** Manzanares-Dauleux MJ, Delourme R, Baron F, Thomas G. Mapping of one major gene and  
901 of QTLs involved in resistance to clubroot in *Brassica napus*. Theor Appl Genet. 2000a;101:  
902 885-891. doi:10.1007/s001220051557.  
903  
904 **38.** R Core Team. A Language and environment for statistical computing. Available from:  
905 <https://www.R-project.org/>.  
906  
907 **39.** Bates DM. lme4: Mixed-effects modeling with R. 2010. Available from: [http://lme4.r-forge.r-](http://lme4.r-forge.r-project.org)  
908 [project.org](http://lme4.r-forge.r-project.org).  
909  
910 **40.** Lenth RV. Least-squares means: The R package lsmeans. J Stat Softw. 2016;69: 1–33.  
911 doi:10.18637/jss.v069.i01.  
912  
913 **41.** Benjamini Y, Hochberg Y. Controlling the false discovery rate: a practical and powerful  
914 approach to multiple testing. J R Stat Soc. 1995;B57: 289–30.  
915  
916 **42.** Manzanares-Dauleux MJ, Divaret I, Baron F, Thomas G. Evaluation of French *Brassica*  
917 *oleracea* landraces for resistance to *Plasmodiophora brassicae*. Euphytica. 2000b;113: 211–  
918 218. doi:10.1023/A:1003997421340.  
919  
920 **43.** Hervé M. RVAideMemoire: diverse basic statistical and graphical functions. R package version  
921 0.9-6. 2017. Available from: <http://CRAN.R-project.org/package=RVAideMemoire>.  
922  
923 **44.** Plassart P, Terrat S, Thomson B, Griffiths R, Decquiedt S, Lelievre M, et al. Evaluation of the  
924 ISO standart 11063 DNA extraction procedure for assessing soil microbial abundance and  
925 community structure. PloS ONE. 2012;7: e44279. doi:10.1371/journal.pone.0044279.  
926  
927 **45.** Chelius MK, Triplett EW. The diversity of archaea and bacteria in association with the roots of  
928 *Zea mays* L.. Microb Ecol. 2001;41: 252–263. doi:10.1007/s002480000087.  
929  
930 **46.** Bodenhausen N, Horton MW, Bergelson J. Bacterial communities associated with the leaves  
931 and the roots of *Arabidopsis thaliana*. PLoS One. 2013;8: e56329.  
932 doi:10.1371/journal.pone.0056329.  
933  
934 **47.** Borneman J, Hartin RJ. PCR primers that amplify fungal rRNA genes from environmental  
935 samples. Appl Environ Microbiol. 2000;66: 4356–60.  
936  
937 **48.** Lê Van A, Quaiser A, Duhamel M, Michon-Coudouel S, Dufresne A, Vandenkoornhuyse P.  
938 Ecophylogeny of the endospheric root fungal microbiome of co-occurring *Agrostis*  
939 *stolonifera*. PeerJ. 2017;5: e3454. doi:10.7717/peerj.3454.  
940

- 941 49. Terrat S, Christen R, Dequiedt S, Lelièvre M, Nowak V, Regnier T, et al. Molecular biomass  
942 and meta taxogenomic assessment of soil microbial communities as influenced by soil DNA  
943 extraction procedure. *Microb Biotechnol.* 2012;5: 135–141. doi:10.1111/j.1751-  
944 7915.2011.00307.x.
- 945
- 946 50. Terrat S, Dequiedt S, Horrigue W, Lelievre M, Cruaud C, Saby NPA, et al. Improving soil  
947 bacterial taxa–area relationships assessment using DNA meta-barcoding. *Heredity.* 2015;114:  
948 468–475. doi:10.1038/hdy.2014.91.
- 949
- 950 51. Cole JR, Wang Q, Cardenas E, Fish J, Chai B, Farris RJ, et al. The Ribosomal database project:  
951 improved alignments and new tools for rRNA analysis. *Nucleic Acids Res.* 2009;37: D141–  
952 D145. doi:10.1093/nar/gkn879.
- 953
- 954 52. Quast C, Pruesse E, Yilmaz P, Gerken J, Schweer T, Yarza P, et al. The SILVA ribosomal RNA  
955 gene database projects: improved data processing and web-based tools. *Nucleic Acids Res.*  
956 2013;37: D590–D596. doi:10.1093/nar/gks1219.
- 957
- 958 53. Oksanen J, Blanchet G, Friendly M, Kindt R, Legendre P, McGlenn D, et al. *Vegan: Community  
959 Ecology Package.* R package version 2.4-3. 2017. Available from: [http://CRAN.R-  
960 project.org/package=vegan](http://CRAN.R-project.org/package=vegan).
- 961
- 962 54. Anderson MJ, Willis TJ. Canonical analysis of principal coordinates: a useful method of  
963 constrained ordination for ecology. *Ecology.* 2003;84: 511–525. doi :10.1890/0012-9658.
- 964
- 965 55. Dombrowski N, Schlaeppi K, Agler MT, Hacquard S, Kemen E, Garrido-Oter R, et al. Root  
966 microbiota dynamics of perennial *Arabidopsis alpina* are dependent on soil residence time but  
967 independent of flowering time. *ISME J.* 2016;11: 43–55. doi:10.1038/ismej.2016.109.
- 968
- 969 56. Robinson MD, McCarthy DJ, Smyth GK. edgeR: a Bioconductor package for differential  
970 expression analysis of digital gene expression data. *Bioinformatics.* 2010;26: 139–140.  
971 doi:10.1093/bioinformatics/btp616.
- 972
- 973 57. Anders S, McCarthy DJ, Chen Y, Okoniewski M, Smyth GK, Huber W, et al. Count-based  
974 differential expression analysis of RNA sequencing data using R and Bioconductor. *Nat  
975 Protoc.* 2013;8: 1765–1786. doi:10.1038/nprot.2013.099.
- 976
- 977 58. Robinson MD, Oshlack A. A scaling normalization method for differential expression analysis  
978 of RNA-seq data. *Genome Biol.* 2010;11: R25. doi:10.1186/gb-2010-11-3-r25.
- 979
- 980 59. de Souza RSC, Okura VK, Armanhi JSL, Jorrín B, Lozano N, da Silva MJ, et al. Unlocking the  
981 bacterial and fungal communities assemblages of sugarcane microbiome. *Sci Rep.* 2016;6:  
982 28774. doi:10.1038/srep28774.
- 983
- 984 60. Niu B, Paulson JN, Zheng X, Kolter R. Simplified and representative bacterial community of  
985 maize roots. *Proc Natl Acad Sci USA.* 2017;114: E2450–E2459.  
986 doi:10.1073/pnas.1616148114.
- 987
- 988 61. Monreal CM, Zhang J, Koziel S, Vidmar J, Gonzalez M, Matus F, et al. Bacterial community  
989 structure associated with the addition of nitrogen and the dynamics of soluble carbon in the  
990 rhizosphere of canola (*Brassica napus*) grown in a Podzol. *Rhizosphere.* 2018;5: 16–25.  
991 doi:10.1016/j.rhisph.2017.11.004.
- 992

- 993       **62.** Rathore R, Dowling DN, Forristal PD, Spink J, Cotter PD, Bulgarelli D, et al. Crop establishment  
994       practices are a driver of the plant microbiota in winter oilseed rape (*Brassica napus*). Front  
995       Microbiol. 2017;8: 1489. doi:10.3389/fmicb.2017.01489.  
996
- 997       **63.** Gkarmiri K, Mahmood S, Ekblad A, Alström S, Högberg N, Finlay R. Identifying the active  
998       microbiome associated with roots and rhizosphere soil of oilseed rape. Appl Environ  
999       Microbiol. 2017;83: e01938-17. doi:10.1128/AEM.01938-17.  
1000
- 1001       **64.** de Compos SB, Youn J-W, Farina R, Jaenicke S, Jünemann S, Szczepanowski R, et al. Changes  
1002       in root bacterial communities associated to two different development stages of Canola  
1003       (*Brassica napus* L. var *oleifera*) evaluated through next-generation sequencing technology.  
1004       Microb Ecol. 2013;65 :593–601. doi:10.1007/s00248-012-0132-9.  
1005
- 1006       **65.** Tkacz A, Cheema J, Chandra G, Grant A, Poole PS. Stability and succession of the rhizosphere  
1007       microbiota depends upon plant type and soil composition. ISME J. 2015;9: 2349–2359.  
1008       doi:10.1038/ismej.2015.41.  
1009
- 1010       **66.** Hartwright LM, Hunter PJ, Walsh JA. A comparison of *Olpidium* isolates from a range of host  
1011       plants using internal transcribed spacer sequence analysis and host range studies. Fungal  
1012       Biol. 2010;114: 26–33. doi :10.1016/j.mycres.2009.09.008.  
1013
- 1014       **67.** Hilton S, Bennett AJ, Keane G, Bending GD, Chandler D, Stobart R, et al. Impact of shortened  
1015       crop rotation of oilseed rape on soil and rhizosphere microbial diversity in relation to yield  
1016       decline. PLoS One. 2013;8: e59859. doi:10.1371/journal.pone.0059859.  
1017
- 1018       **68.** Hacquard S, Kracher B, Hiruma K, Münch PC, Garrido-Oter R, Thon MR et al. Survival trade-  
1019       offs in plant roots during colonization by closely related beneficial and pathogenic fungi. Nat  
1020       Commun. 2016;7: 11362. doi: 10.1038/ncomms11362.  
1021
- 1022       **69.** Erlacher A, Cardinale M, Grosch R, Grube M, Berg G. The impact of the pathogen *Rhizoctonia*  
1023       *solani* and its beneficial counterpart *Bacillus amyloliquefaciens* on the indigenous lettuce  
1024       microbiome. Front Microbiol. 2014;5: 175. doi:10.3389/fmicb.2014.00175.  
1025
- 1026       **70.** Wei Z, Hu J, Gu Y, Yin S, Xu Y, Jousset A, et al. *Ralstonia solanacearum* pathogen disrupts  
1027       bacterial rhizosphere microbiome during an invasion. Soil Biol Biochem 2018;118: 8–17.  
1028       doi:10.1016/j.soilbio.2017.11.012.  
1029
- 1030       **71.** Lemarié S, Robert-Seilaniantz A, Lariagon C, Lemoine J, Marnet N, Jubault M et al. Both the  
1031       jasmonic acid and the salicylic acid pathways contribute to resistance to the biotrophic  
1032       clubroot agent *Plasmodiophora brassicae* in *Arabidopsis*. Plant Cell Physiol. 2015;56: 2158–  
1033       68. doi:10.1093/pcp/pcv127.  
1034
- 1035       **72.** Lebeis SL, Paredes SH, Lundberg DS, Breakfield N, Gehring J, McDonald M et al. Salicylic acid  
1036       modulates colonization of the root microbiome by specific bacterial taxa. Science. 2015;349:  
1037       860–4. doi:10.1126/science.aaa8764.  
1038
- 1039       **73.** Carvalhais LC, Dennis PG, Badri DV, Kidd BN, Vivanco JM, Schenk PM. Linking jasmonic acid  
1040       signaling, root exudates, and rhizosphere microbiomes. Mol Plant Microbe Interact. 2015;  
1041       28: 1049–58. doi: 10.1094/MPMI-01-15-0016-R.  
1042
- 1043       **74.** Chapelle E, Mendes R, Bakker PAHM, Raaijmakers JM. Fungal invasion of the rhizosphere  
1044       microbiome. ISME J. 2016;10: 265–268. doi:10.1038/ismej.2015.82.

1045  
1046 **75.** Berendsen RL, Vismans G, Yu K, Song Y, de Jonge R, Burgman WP et al. Disease-induced  
1047 assemblage of a plant-beneficial bacterial consortium. *ISME J.* 2018;12: 1496–1516. doi:  
1048 10.1038/s41396-018-0093-1.

1049

## 1050 **Supporting information**

1051 **S1 Fig. Alpha diversity of bacterial communities from non-inoculated (NI) plants.** Richness (i.e.  
1052 observed OTU) and diversity (i.e. Shannon index) of non-inoculated root (R), rhizosphere (RS) and  
1053 bulk soil (BS) samples at different sampling dates are represented. Bacterial diversities were  
1054 estimated with OTUs count data normalized by sample size and rarefied to 1,000 counts. Sampling  
1055 date refers to 10 (T1), 24 (T3) and 45 (T5) days after sowing (DAS). For each sample, the number of  
1056 replicates was  $n = 3$ . At each sampling date, lowercase letters indicate significant differences ( $p$ -  
1057 values  $\leq 0.05$ ) between conditions, which were assessed by ANOVA followed by post hoc Tukey's HSD  
1058 test.

1059 **S2 Fig. Alpha diversity of fungal communities from non-inoculated (NI) plants.** Richness (i.e.  
1060 observed OTU) and diversity (i.e. Shannon index) of non-inoculated root (R), rhizosphere (RS) and  
1061 bulk soil (BS) samples at different sampling dates are represented. Fungal diversities were estimated  
1062 with OTUs count data normalized by sample size and rarefied to 1,000 counts. Sampling date refers  
1063 to 10 (T1), 24 (T3) and 45 (T5) days after sowing (DAS). For each sample, the number of replicates  
1064 was  $n = 3$ . At each sampling date, lowercase letters indicate significant differences ( $p$ -values  $\leq 0.05$ )  
1065 between conditions, which were assessed by ANOVA followed by post hoc Tukey's HSD test.

1066 **S3 Fig. Unconstrained Principal Coordinate Analysis (PcoA) of the bacterial and fungal communities**  
1067 **from non-inoculated Chinese cabbage plants and bulk soil samples.** The variances explained by  
1068 PCoA axes are given in parenthesis. Compartment refers to bulk soil (BS), rhizosphere soil (RS) and

1069 roots (R), represented by orange, brown and green colours, respectively. Sampling date refers to 10  
1070 (T1), 24 (T3) and 45 (T5) days after sowing (DAS).

1071

1072 **S4 Fig. Constrained Principal Coordinate Analysis (CPCoA) of the bacterial and fungal communities**  
1073 **from non-inoculated Chinese cabbage plants and bulk soil samples.** Compartment refers to bulk soil  
1074 (BS), rhizosphere soil (RS) and roots (R), represented by orange, brown and green colours,  
1075 respectively. Sampling date refers to 10 (T1), 24 (T3) and 45 (T5) days after sowing (DAS),  
1076 represented by crosses, triangles and squares respectively. The variances explained by CPCoA axes  
1077 are given in parenthesis. For each CPCoA, variations between samples in Bray-Curtis distances were  
1078 constrained by compartment (in the left column) or sampling date (in the right column) factor.  
1079 Canonical analysis of principal coordinates (CAP) was performed to quantify the influence of these  
1080 factors on the  $\beta$ -diversity. The percentage of variation refers to the fraction of the total variance of  
1081 the data explained by each constrained factor. The p-values indicate if the influence of each of these  
1082 constrained factors on the  $\beta$ -diversity was significant ( $p$ -values  $\leq 0.05$ ).

1083

1084 **S5 Fig. Alpha diversity of bacterial communities from inoculated (I) compared to non-inoculated**  
1085 **(NI) plants.** Richness (i.e. observed OTU) and diversity (i.e. Shannon index) of root (R) and  
1086 rhizosphere (RS) samples from NI and I plants were measured at different sampling dates. Bacterial  
1087 diversity was estimated with OTUs count data normalized by sample size and rarefied to 1,000  
1088 counts. Richness and diversity associated NI plants and plants inoculated by *P. brassicae* (I) at each  
1089 sampling date (T1 to T5) were compared. Sampling date refers to 0 (T1), 7 (T2), 14 (T3), 23 (T4) and  
1090 35 (T5) days after inoculation (DAI) with *P. brassicae*. At each sampling date, lowercase letters  
1091 indicate significant differences ( $p$ -values  $\leq 0.05$ ) between conditions, which were assessed by ANOVA  
1092 followed by post hoc Tukey's HSD test.

1093

1094 **S6 Fig. Alpha diversity of fungal communities from inoculated (I) compared to non-inoculated (NI)**

1095 **plants.** Richness (i.e. observed OTU) and diversity (i.e. Shannon index) of root (R) and rhizosphere

1096 (RS) samples from NI and I plants were measured at different sampling dates. Fungal diversity was

1097 estimated with OTUs count data normalized by sample size and rarefied to 1,000 counts. Richness

1098 and diversity associated to NI and I plants at each sampling date (T1 to T5) were compared. Sampling

1099 date refers to 0 (T1), 7 (T2), 14 (T3), 23 (T4) and 35 (T5) days after inoculation (DAI) with *P. brassicae*.

1100 At each sampling date, lowercase letters indicate significant differences ( $p$ -values  $\leq 0.05$ ) between

1101 conditions, which were assessed by ANOVA followed by post hoc Tukey's HSD test.

1102 **S1 Table. Comparison of bacterial (B) and fungal (F) OTUs relative abundances in the roots (R) and**

1103 **rhizosphere (RS) of healthy and diseased Chinese cabbage plants.** This table is organized into four

1104 tabs corresponding to the description of bacterial OTUs i) from the roots, ii) from the rhizosphere,

1105 fungal OTUs iii) from the roots and iv) from the rhizosphere. Mean values of abundance (expressed in

1106 %) were obtained from three replicates per condition and sampling date. Condition refers to non-

1107 inoculated (NI) and inoculated (I) plants. Sampling date refers to 0 (T1), 7 (T2), 14 (T3), 23 (T4) and 35

1108 (T5) days after inoculation (DAI) by *P. brassicae*. OTUs with relative abundances below 1% were not

1109 shown. Significant differences ( $p$ -values  $\leq 0.05$ ) of OTU frequencies between two samples are

1110 indicated by crosses. For example, T2 NI/I refers to the comparison of each OTU frequencies

1111 between NI and I plants at T2; NI T1/ I T2 refers to the comparison of each OTU frequencies in

1112 communities collected from NI plants at T1 and I plants at T2.

1113

1114 **S2 Table. Quantification of non-inoculated (NI) and inoculated (I) plant traits.** The number of leaves

1115 per plant, the shoot and root fresh weight, the plant leaf areas, the plant height and root length were

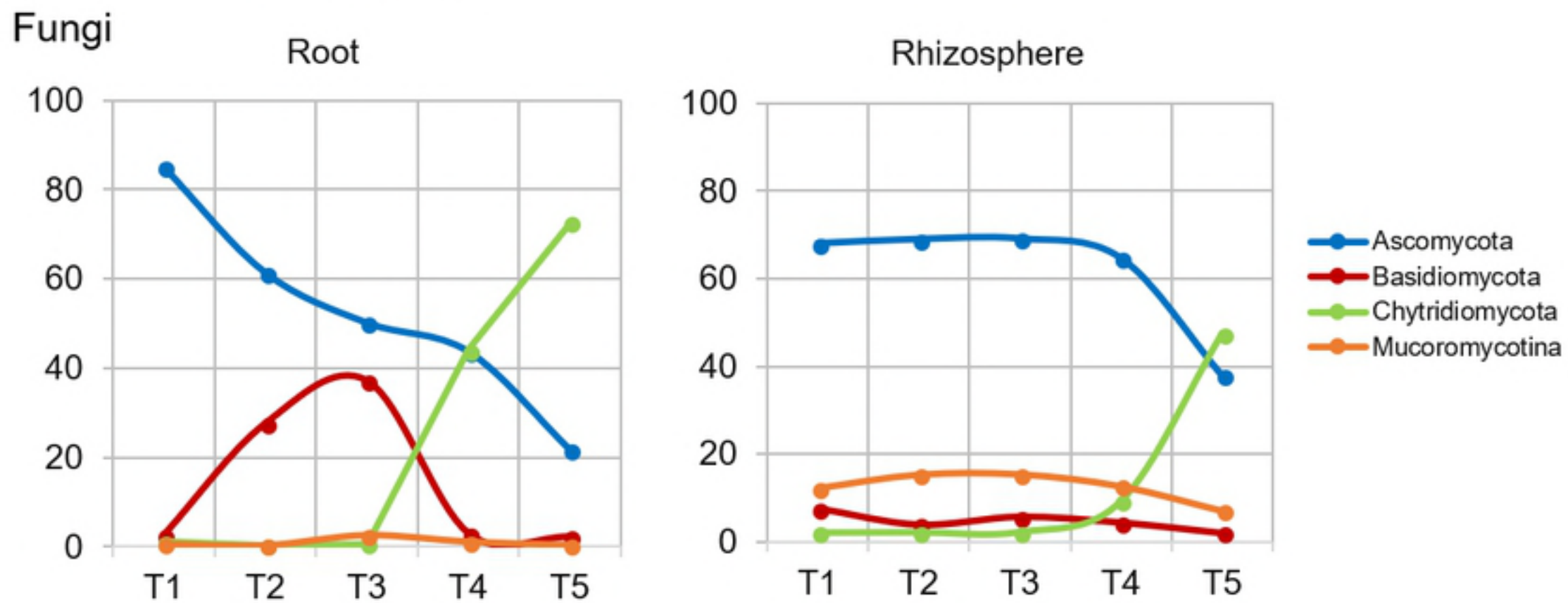
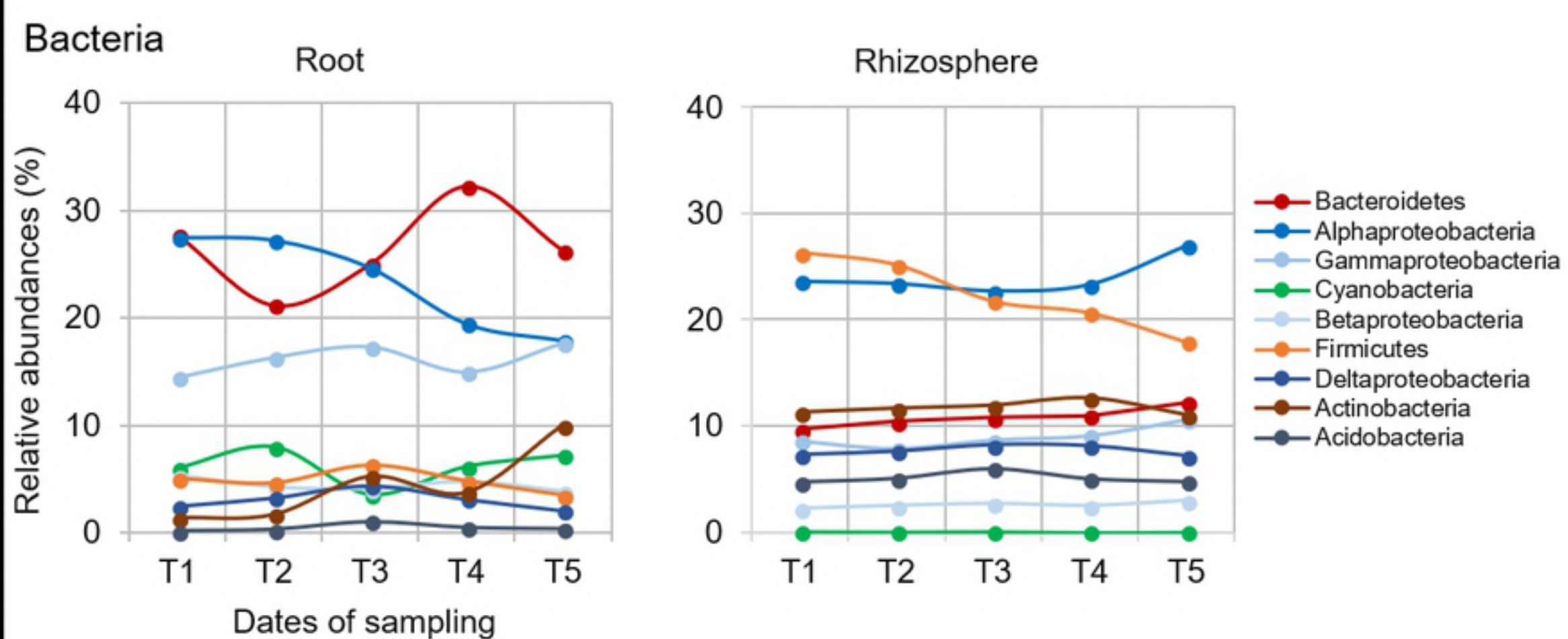
1116 measured during the kinetics of plant growth at 10 (T1), 17 (T2), 24 (T3), 33 (T4) and 45 (T5) days

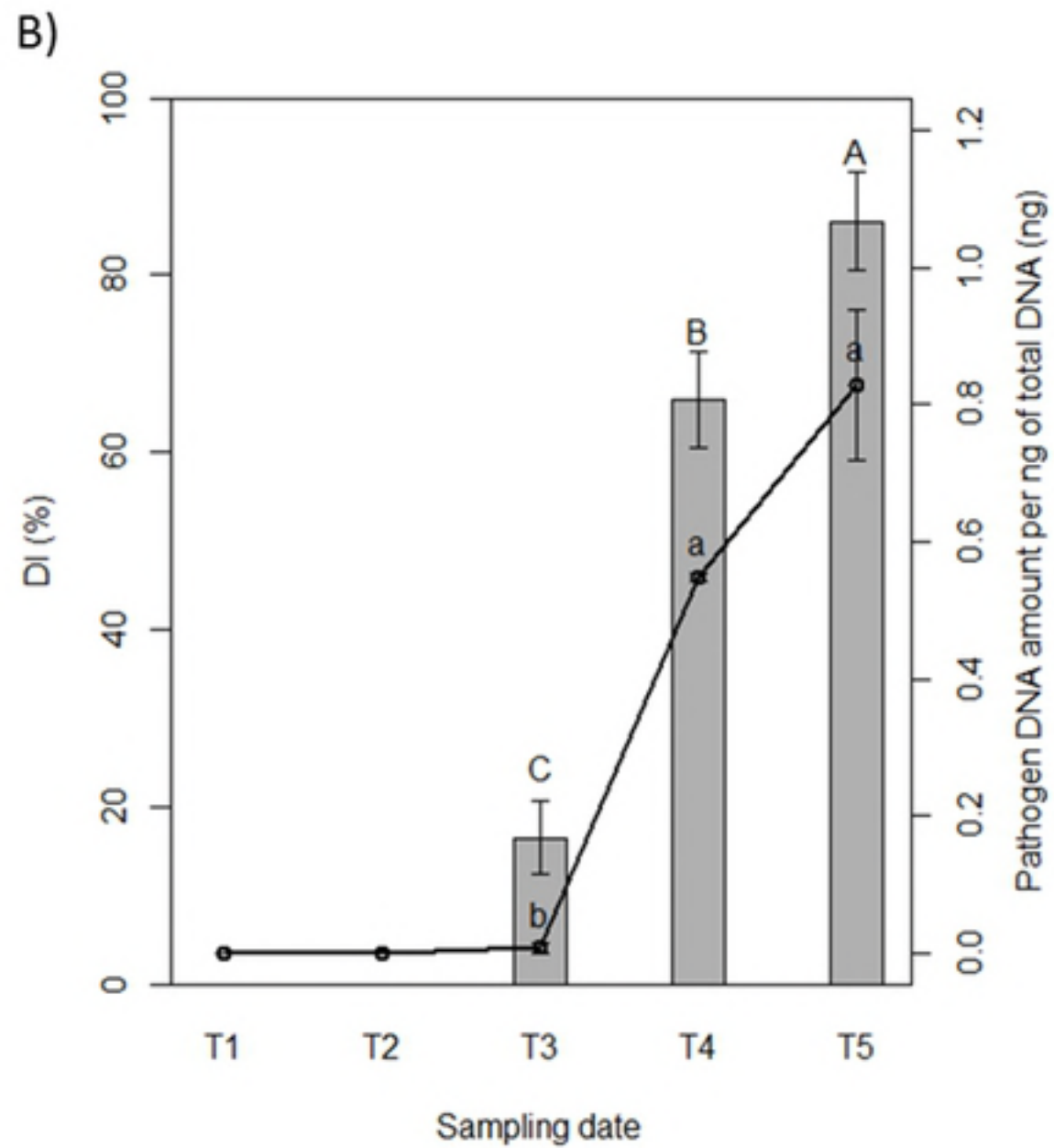
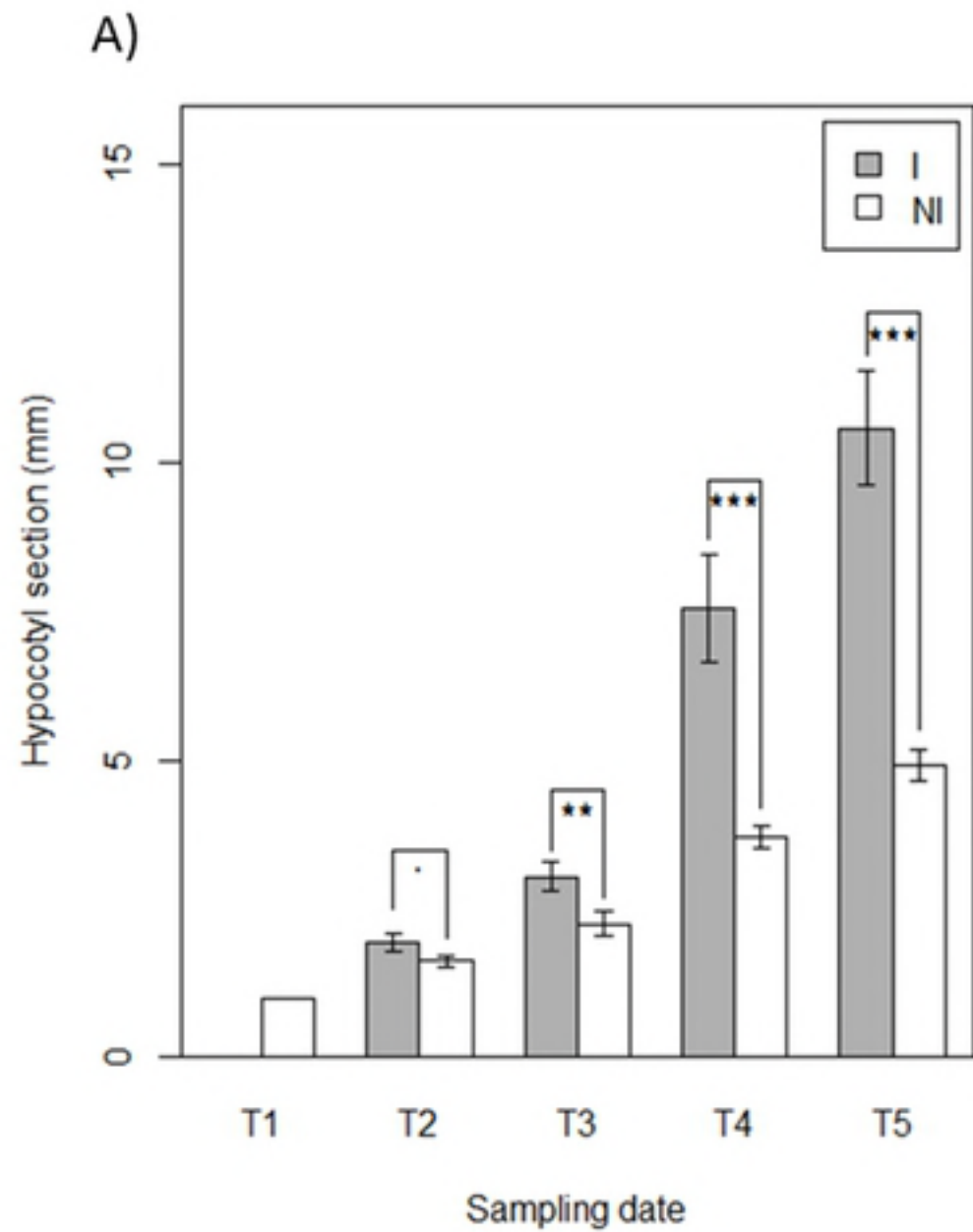
1117 after sowing, corresponding to 0 (T1), 7 (T2), 14 (T3), 23 (T4) and 35 (T5) days after inoculation. At



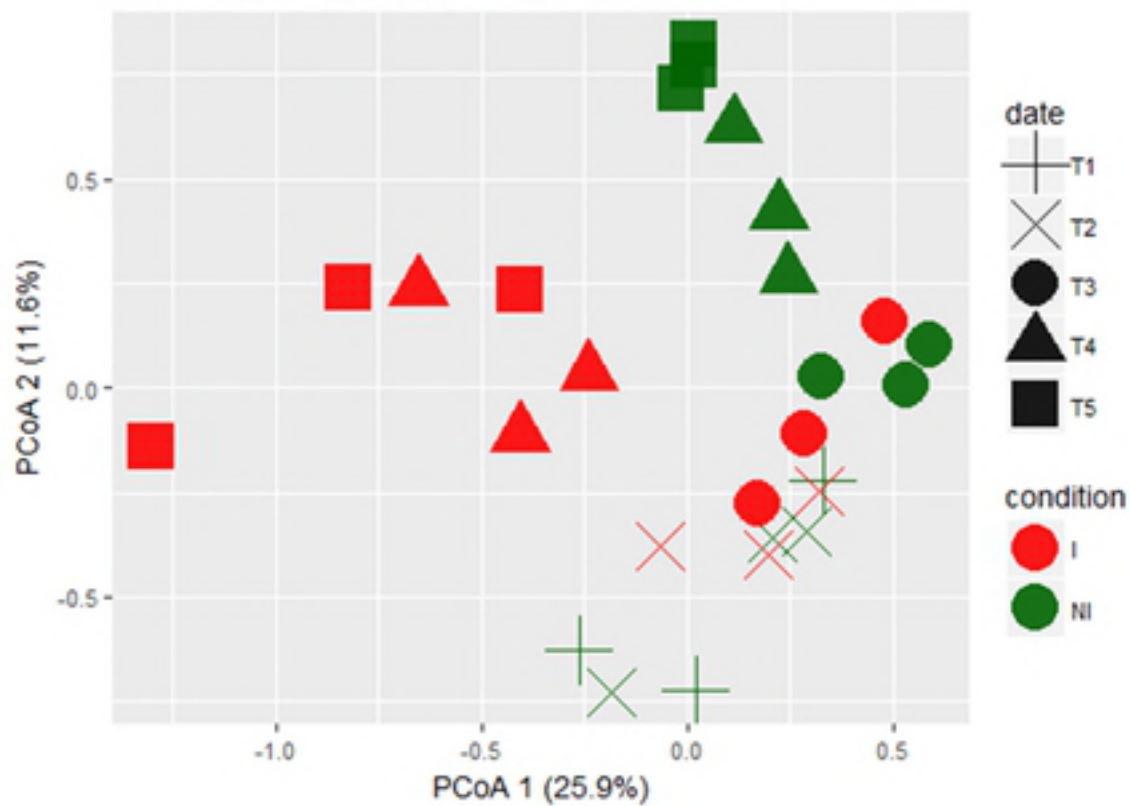
1118 each sampling date, numbers in bold and lowercase letters indicate significant differences ( $p$ -values  $\leq$   
1119 0.05) between inoculated (I) and non-inoculated (NI) plants. SEM: standard error of the mean; nd:  
1120 not determined.

1121

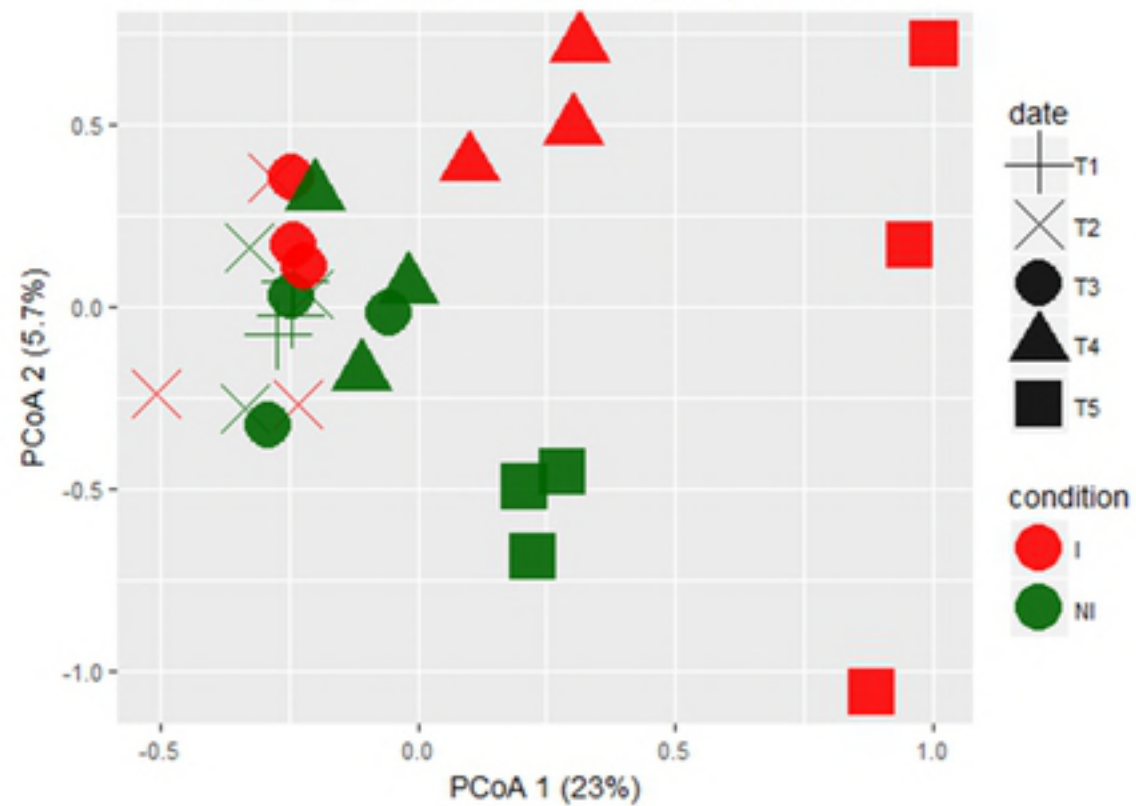




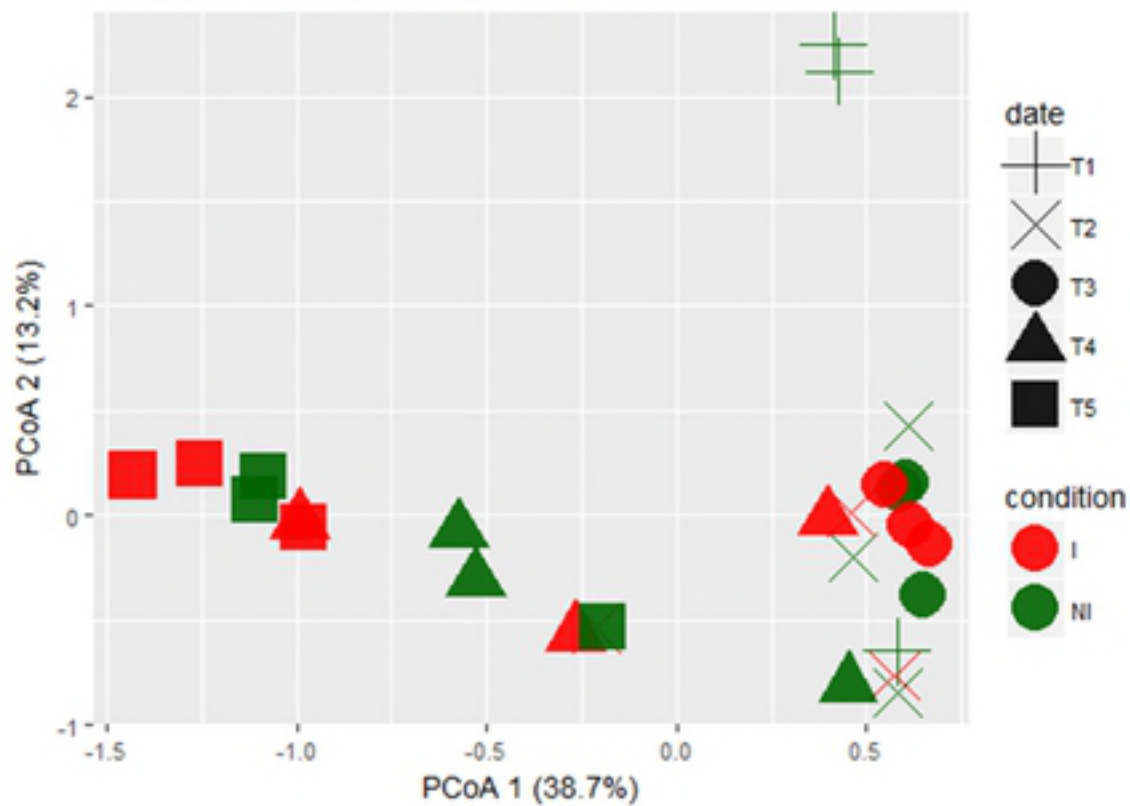
Bacteria\_OTU\_root\_I vs NI\_Bray Curtis



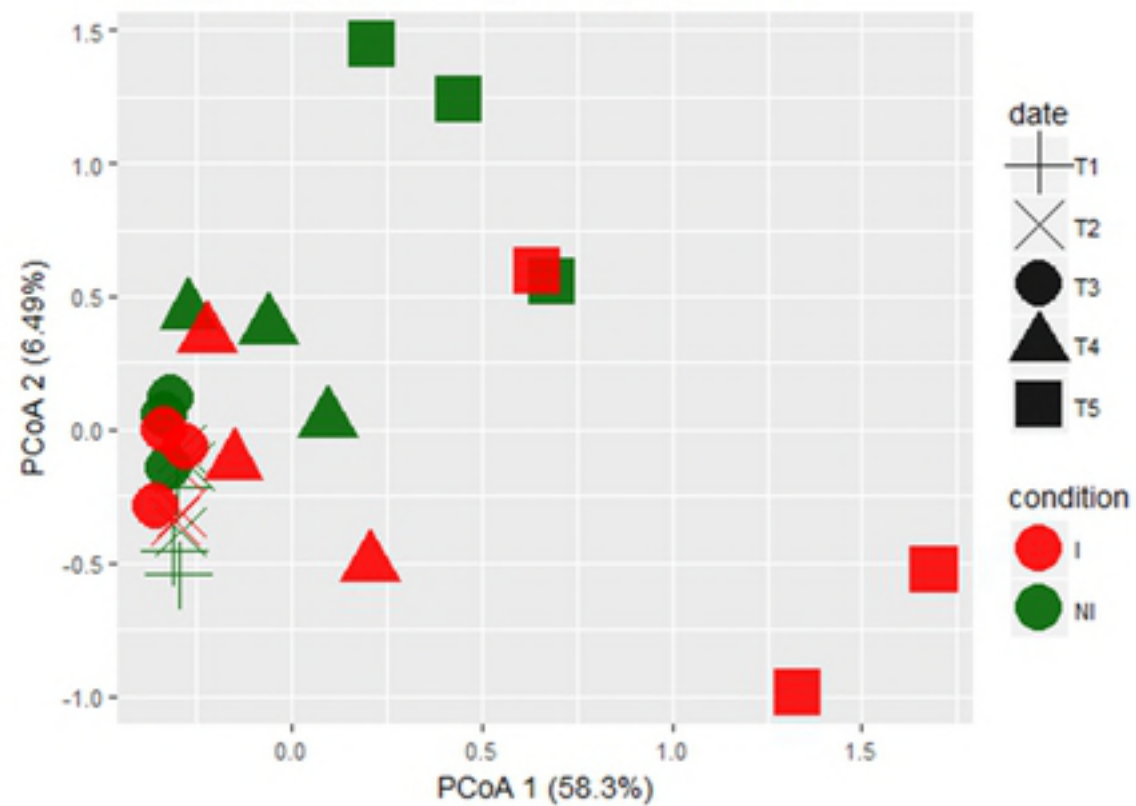
Bacteria\_OTU\_rhizosphere\_I vs NI\_Bray Curtis

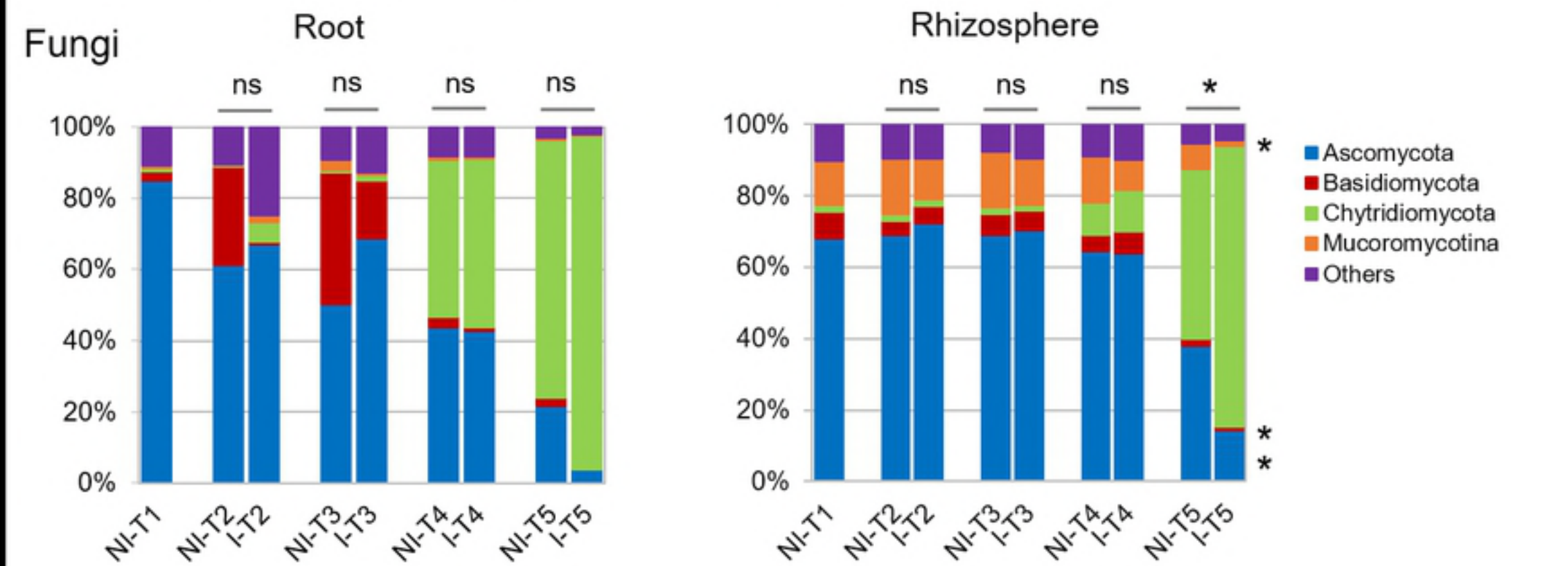
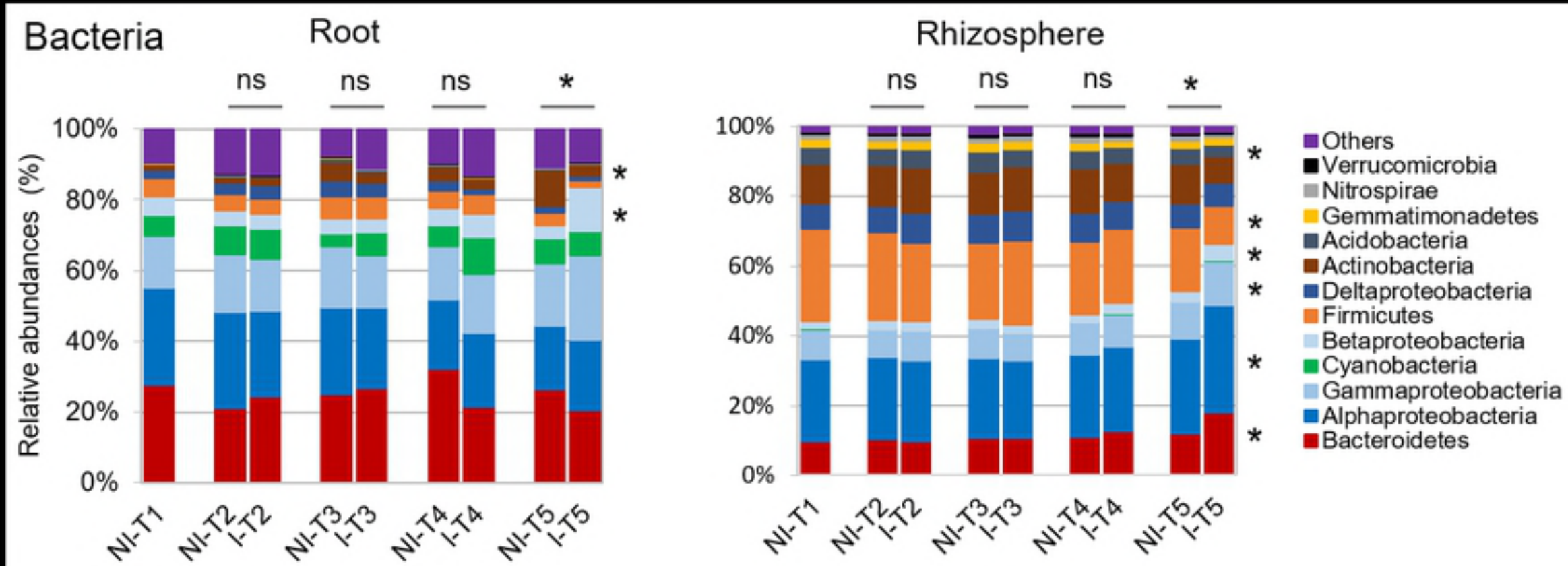


Fungi\_OTU\_root\_I vs NI\_Bray Curtis

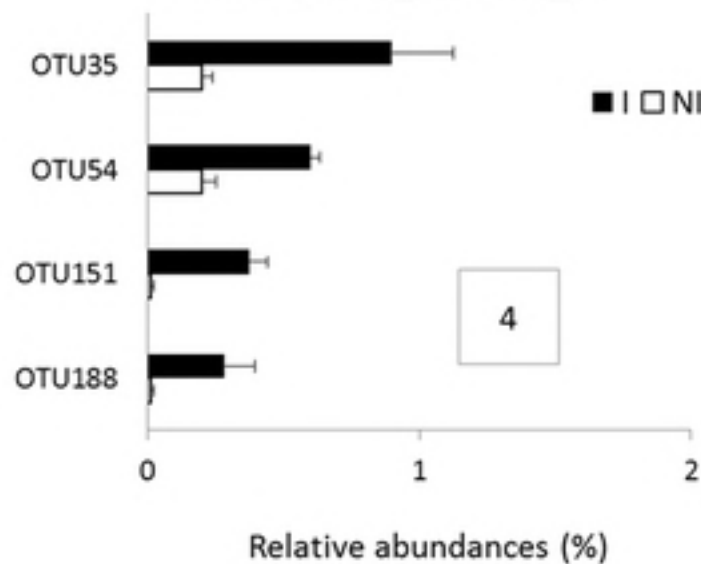


Fungi\_OTU\_rhizosphere\_I vs NI\_Bray Curtis

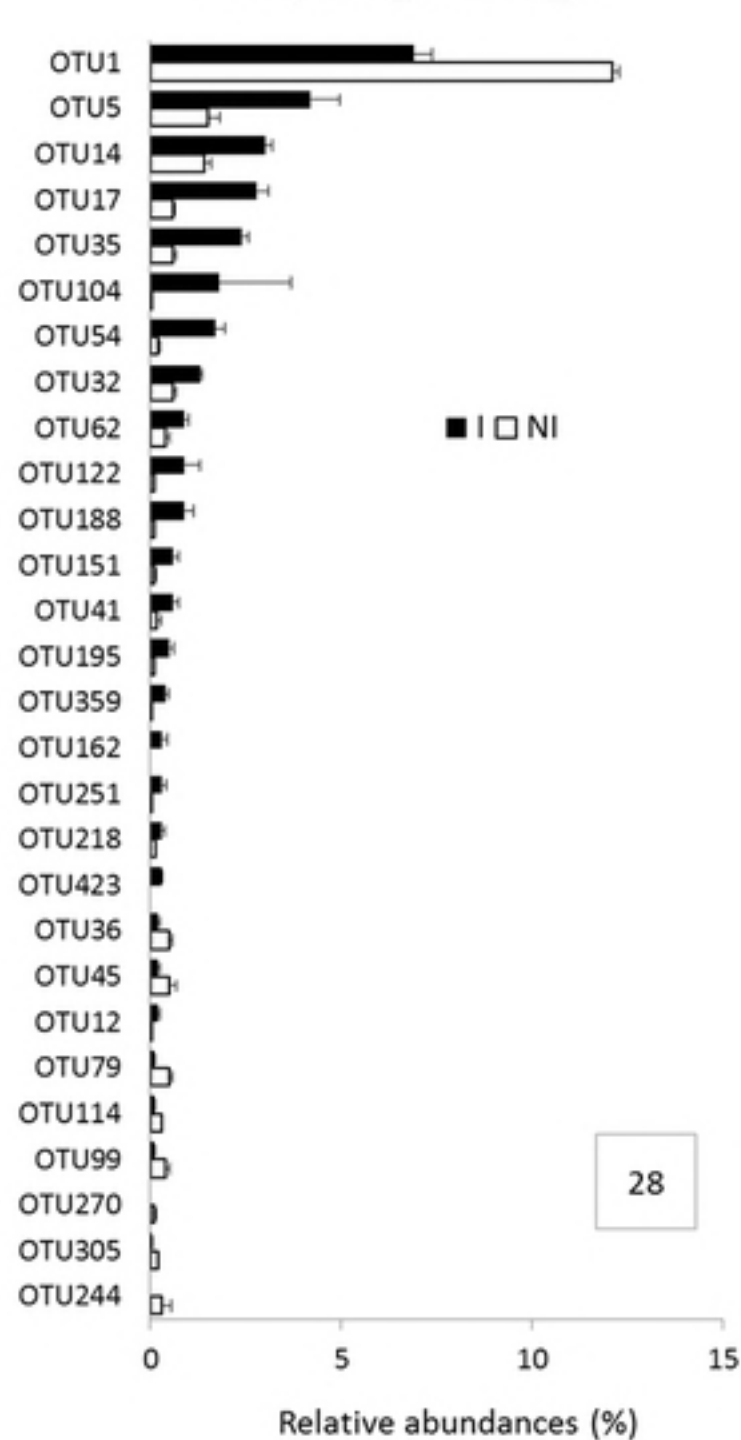




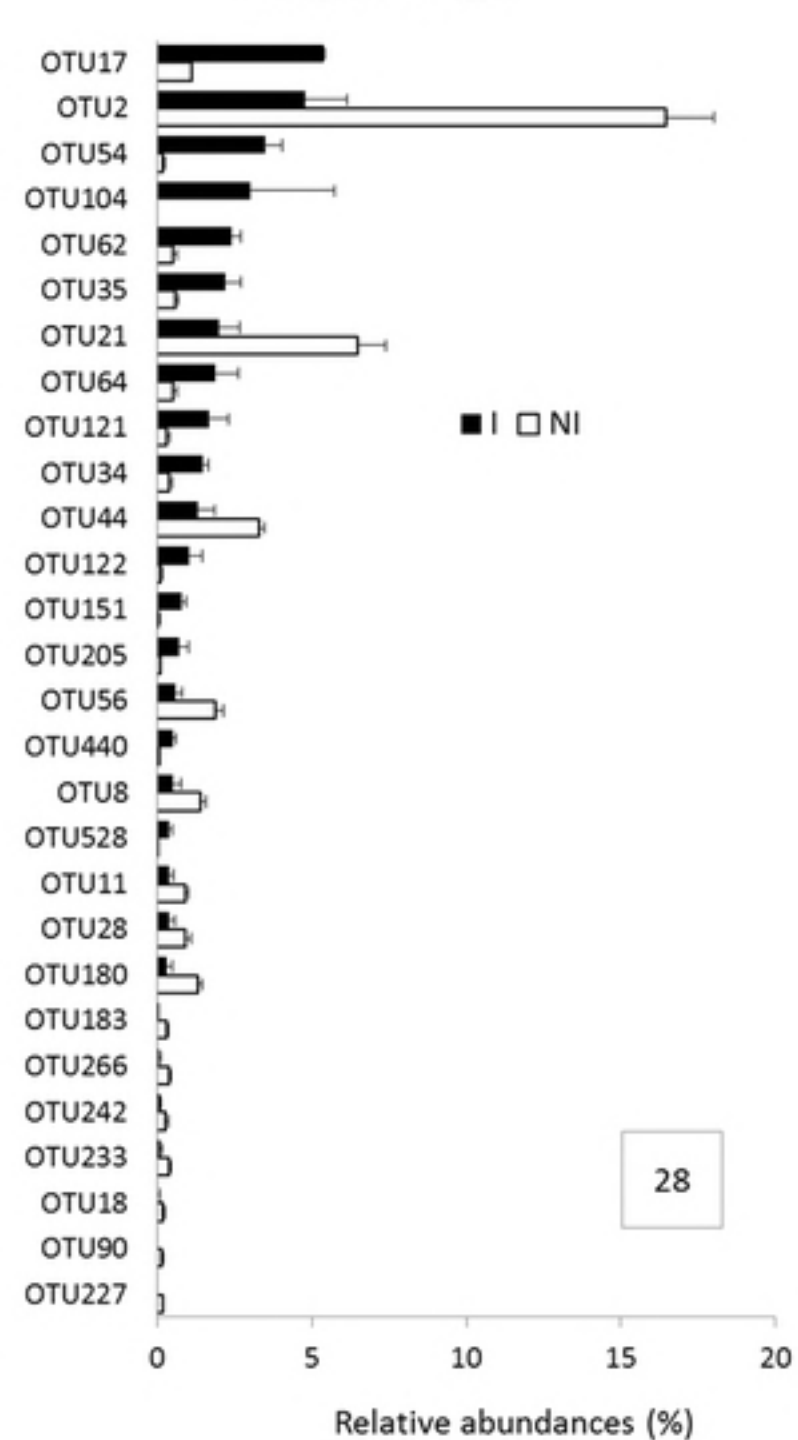
Rhizosphere\_bacteria\_T4



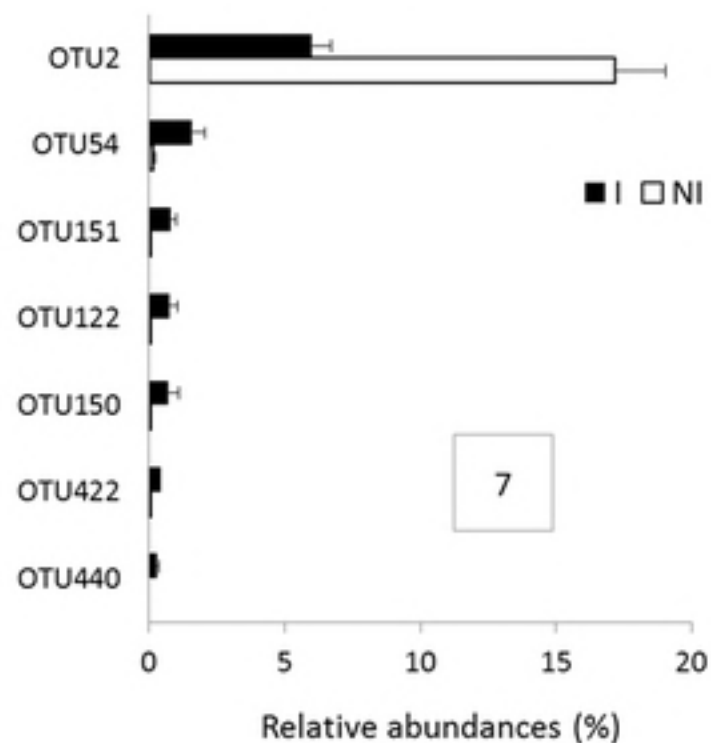
Rhizosphere\_bacteria\_T5

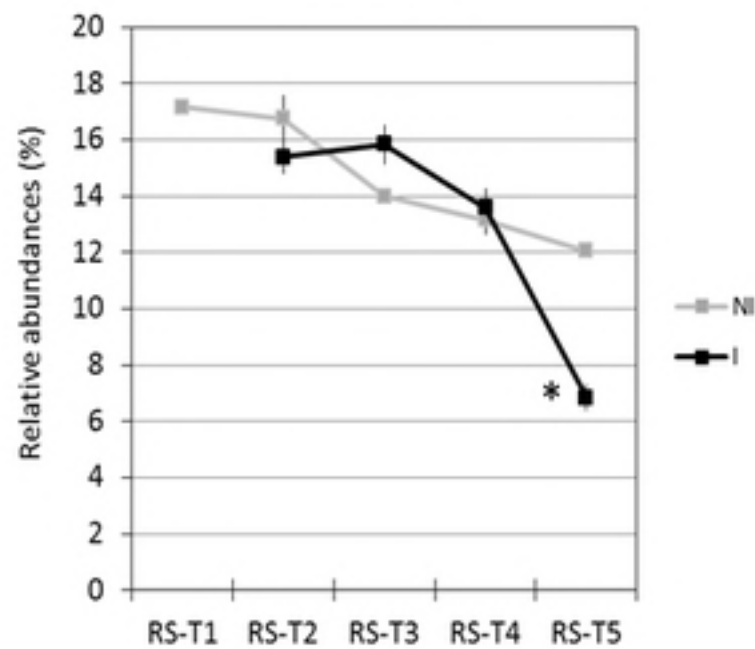
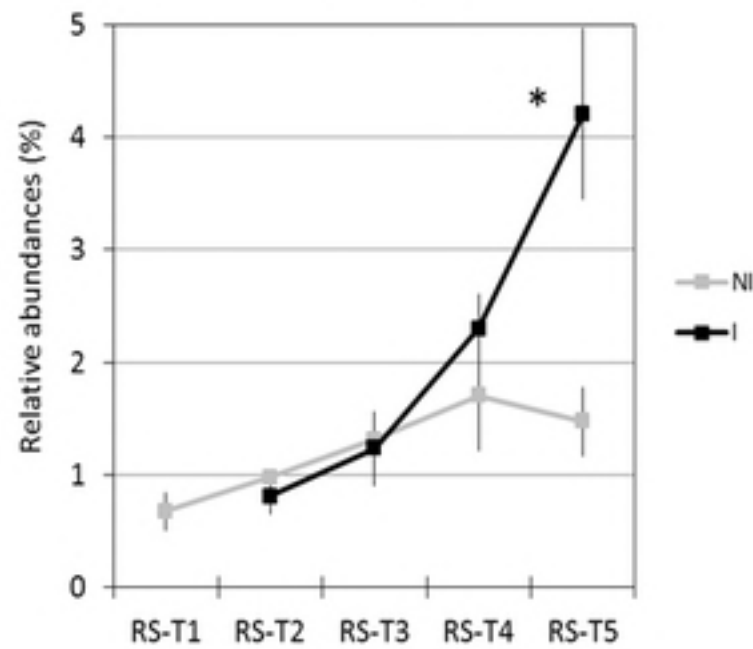
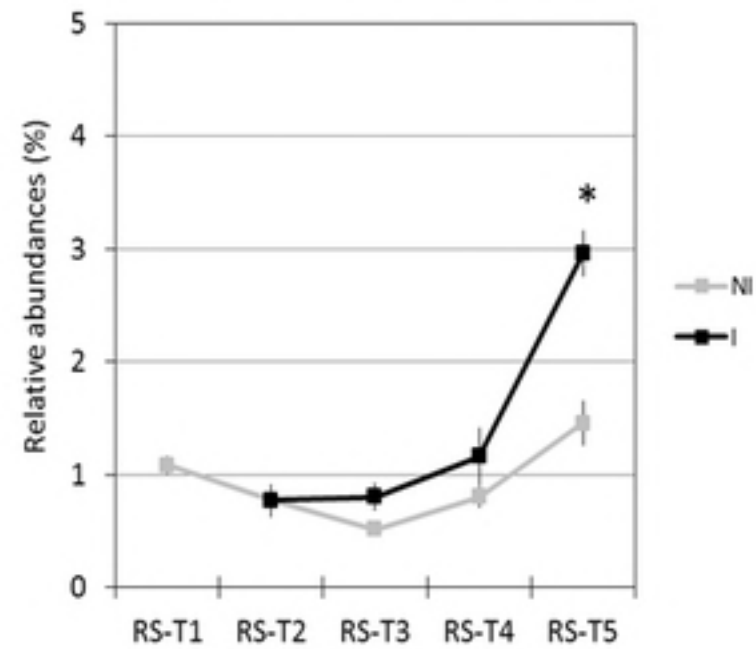
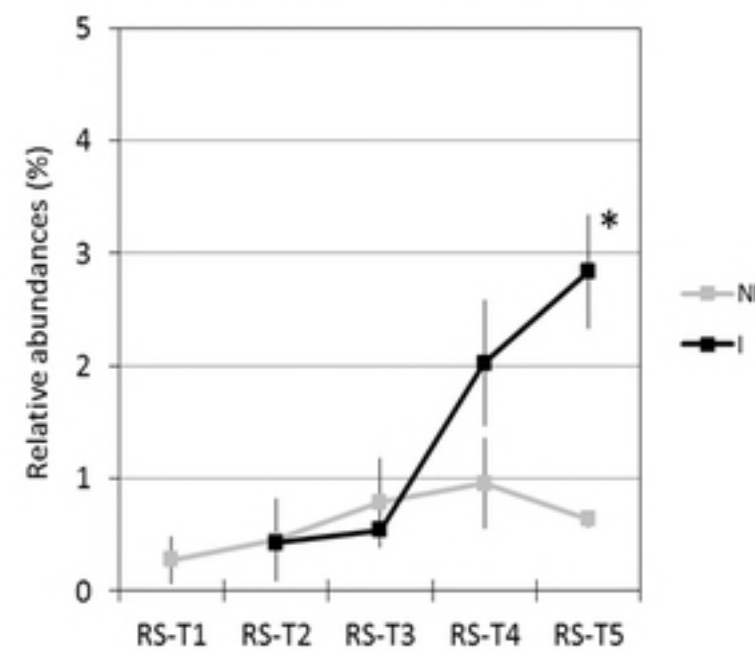
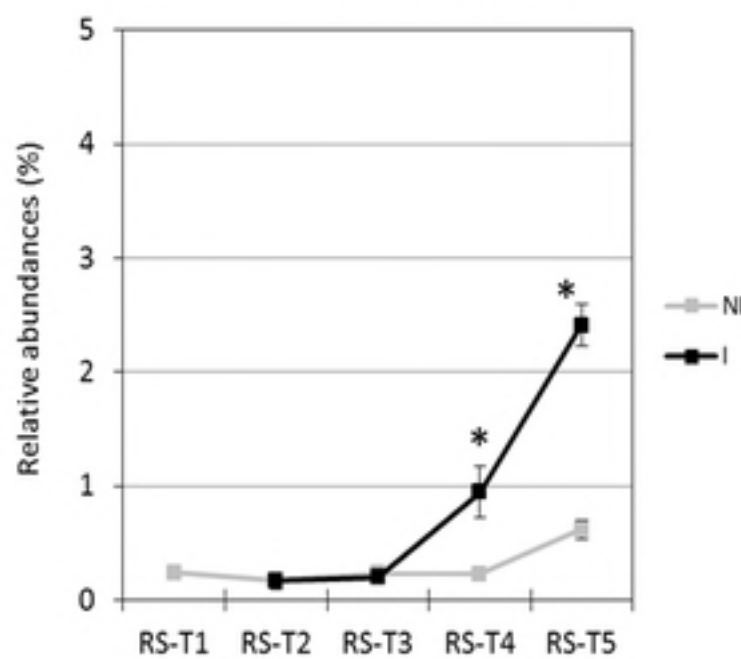
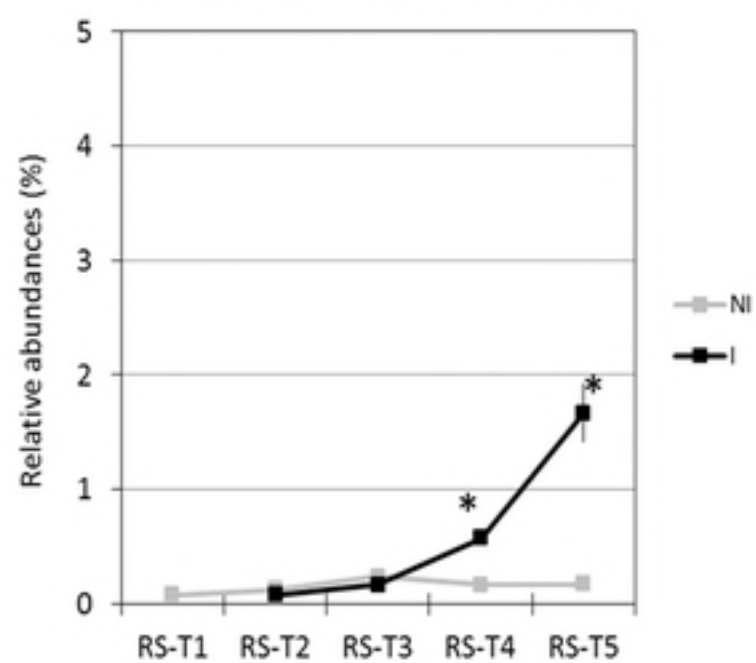


Root\_bacteria\_T5

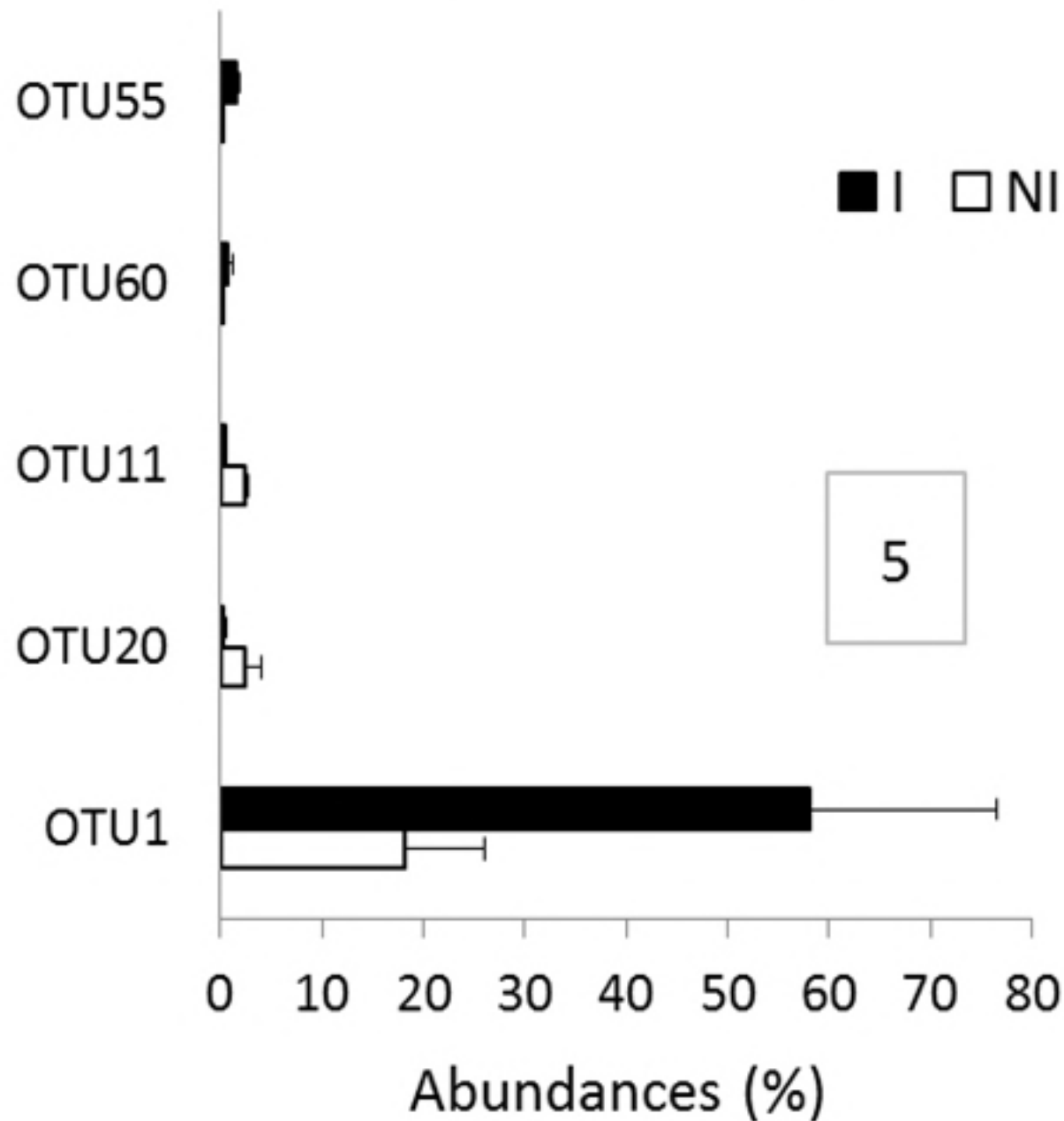


Root\_bacteria\_T4



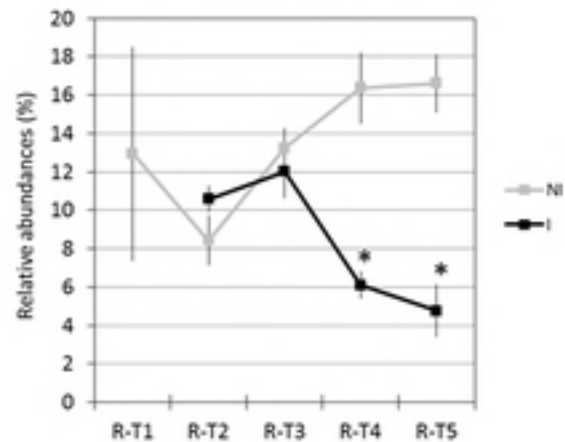
OTU1 (*Bacillus*)OTU5 (*Flavobacterium*)OTU14 (*Dokdonella*)OTU17 (*Pseudomonas*)OTU35 (*Sphingopyxis*)OTU54 (non-assigned  $\beta$ -Proteobacteria)

# Rhizosphere\_fungi\_T5

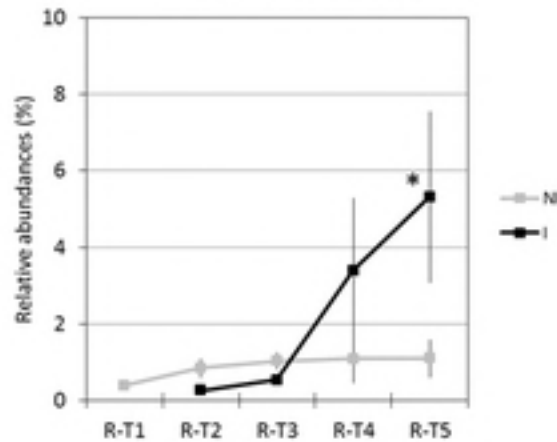




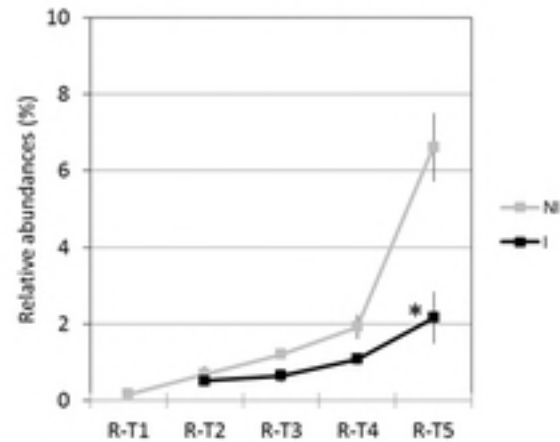
OTU2 (Flavisolibacter)



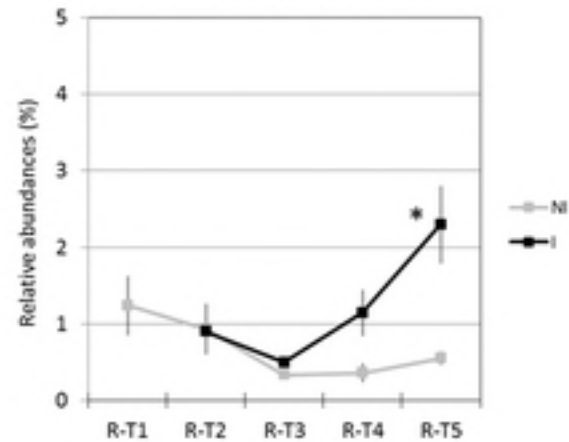
OTU17 (Pseudomonas)



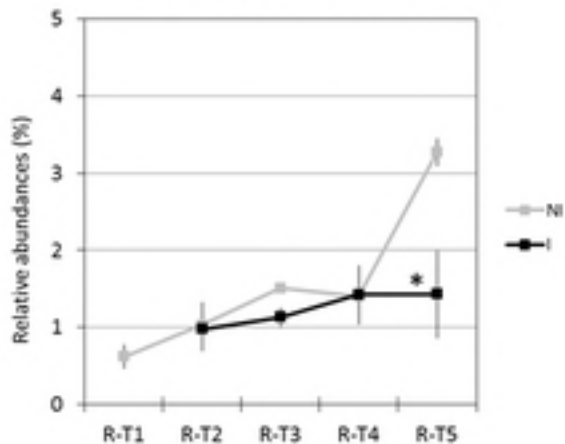
OTU21 (Streptomyces)



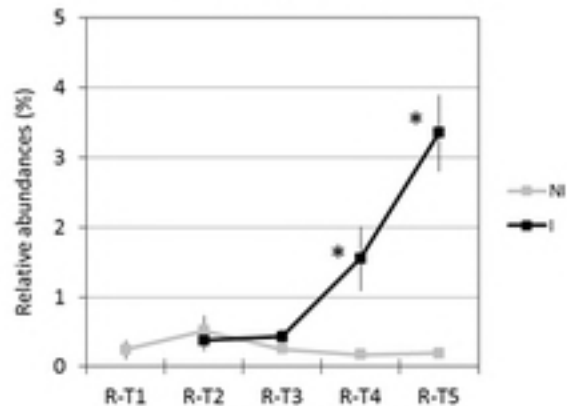
OTU35 (Sphingopyxis)



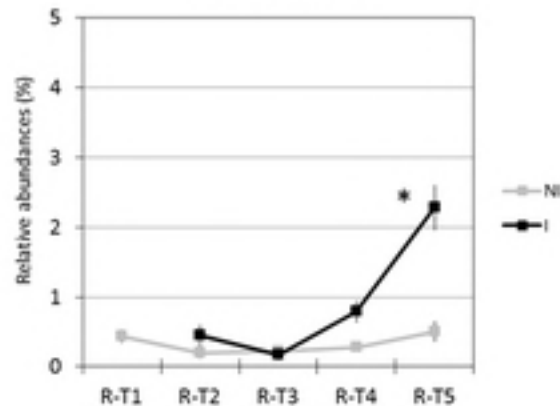
OTU44 (Pseudomonas)

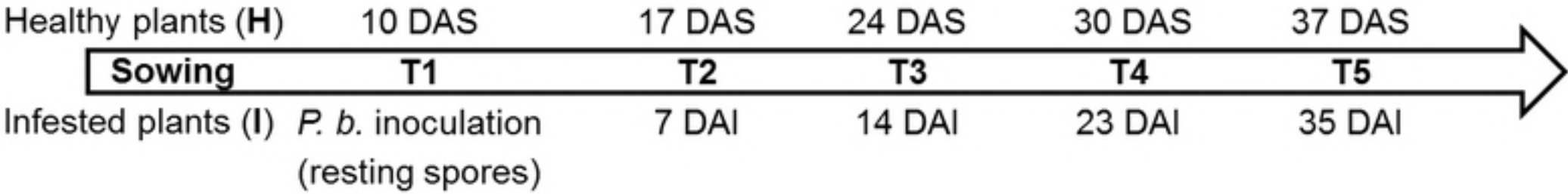


OTU54 (no assigned beta Proteobacteria)

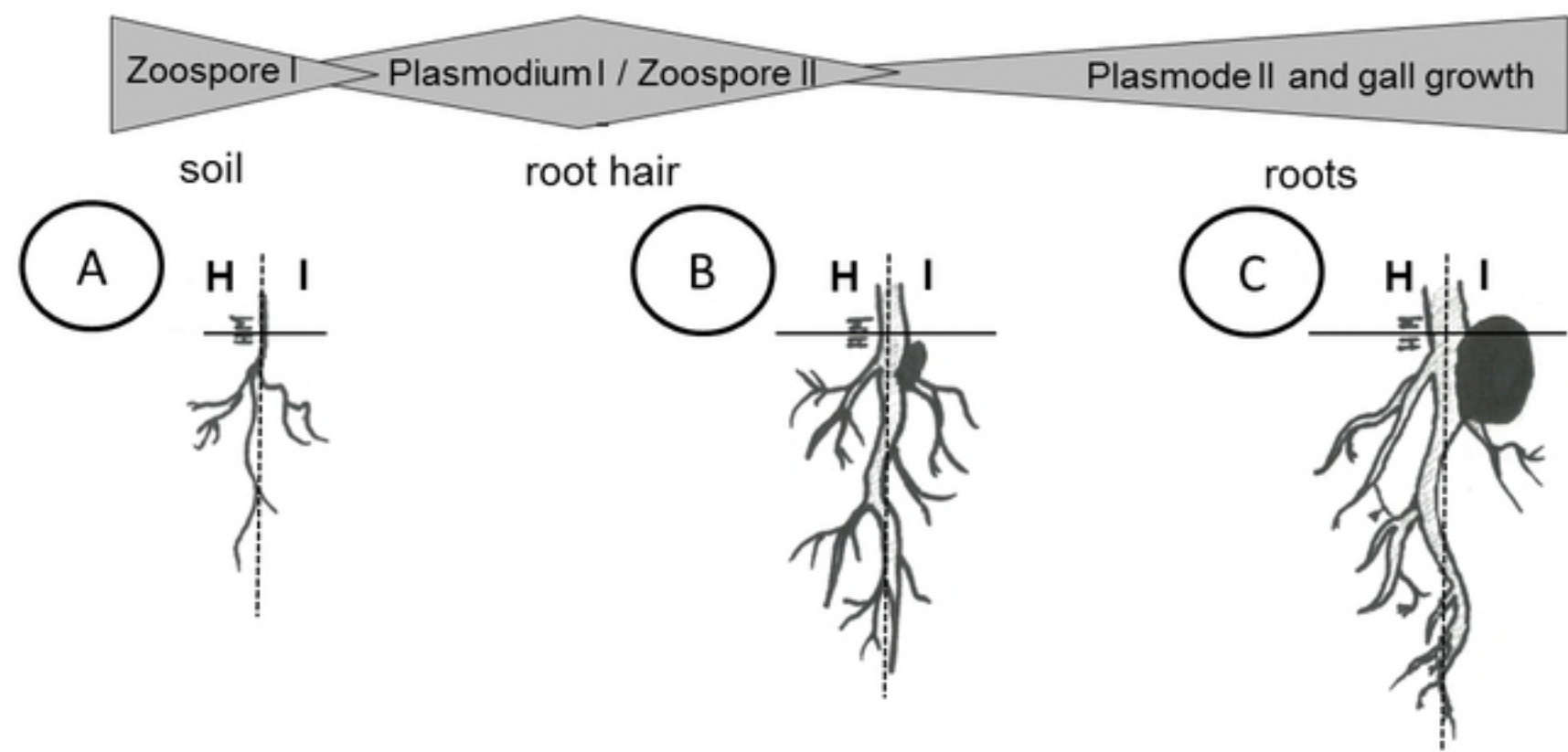


OTU62 (no assigned beta Proteobacteria)





Sampling strategy



Life history traits of *P. brassicae*  
-  
Habitat / plant organs

i. equal production of root metabolites / exudates  
ii. no defense induction

↓

equal microbiota 'diversity' in rhizosphere and roots between H and I plants

i. limited differentiation of root metabolites / exudates  
ii. low defense reaction

↓

close microbiota 'diversity' in rhizosphere and roots between H and I plants

i. strong differentiation of root metabolites / exudates  
ii. high defense reaction

↓

strong microbiota differentiation in root and by extension in rhizosphere between H and I plants

Theoretical framework interactions